IEEE Access
Multidisciplinary ⋮ Rapid Review ⋮ Open Access Journal

Received 30 November 2022, accepted 14 December 2022, date of publication 26 December 2022,
date of current version 3 January 2023.

Digital Object Identifier 10.1109/ACCESS.2022.3232334

RESEARCH ARTICLE

Prediction Error Method (PEM)-Based Howling Cancellation in Hearing Aids: Can We Do Better?

MUHAMMAD TAHIR AKHTAR[1], (Senior Member, IEEE), FELIX ALBU[2], (Senior Member, IEEE), AND AKINORI NISHIHARA[3], (Life Fellow, IEEE)

[1]Department of Electrical and Computer Engineering, School of Engineering and Digital Sciences, Nazarbayev University, Astana 010000, Kazakhstan
[2]Department of Electronics, Valahia University of Târgoviște, 130082 Târgoviște, Romania
[3]Tokyo Institute of Technology, Ookayama, Meguro-ku, Tokyo 152-8552, Japan

Corresponding author: Muhammad Tahir Akhtar (muhammad.akhtar@nu.edu.kz; akhtar@ieee.org)

The work of Felix Albu was supported by the Romanian Ministry of Research, Innovation, and Digitization, National Scientific Research Council (CNCS), the Executive Unit for Financing Higher Education, Research, Development and Innovation (UEFISCDI), through the National Research-Development and Innovation Plan (PNCDI) under Project PN-III-P4-PCE-2021-0780. The work of Akinori Nishihara was supported by Scholarship Donation (Research) by the Tokyo Institute of Technology (Budget code: 11SH201000000000, SH01ZZSH30300040) under Project SH30300040.

ABSTRACT This work develops an effective technique acoustic feedback cancellation (AFC) in the digital hearing aid (DHAid) devices. The normalized least mean square (NLMS) algorithm-based AFC method may suffer from a biased convergence. The biased convergence problem is considerably resolved by the prediction error method (PEM)-based AFC (PEM-AFC); however, it may demonstrate a slow convergence. The proposed method's main structure is based two adaptive filters. The main adaptive AFC filter receives its input from the DHAid receiver signal, while the auxiliary AFC filter is activated by a probe signal. The main idea is to apply a lattice filtering-based pre-processing for decorrelation in the main AFC filter's update equation. This produces a Newton-like adaptive algorithm with fast convergence. Additionally, the lattice filtering is executed on a sample-by-sample basis, in contrast to the frame-based execution in the traditional PEM-AFC method. As the AFC system converges, the level of the probe signal is decreased to improve the output SNR; however, the low-level input signal slows down auxiliary AFC filter's convergence. In order to improve the convergence speed, the gradient information from a maximum Versoria-criterion (MVC) is incorporated into the auxiliary AFC filter's update algorithm. The two adaptive filters' coefficients are exchanged, to ensure that both adaptive filters converge to a good estimate of the true acoustic feedback path. Simulations show that the proposed method works well for speech/signals and for DHAid devices with different gain settings. Additionally, the proposed method shows robust performance in the event of a sudden change in the acoustic environment.

INDEX TERMS Normalized LMS algorithm, lattice adaptive filtering, digital hearing aid devices, acoustic feedback cancellation.

I. INTRODUCTION

Thanks to advancements in medicine and medical support and infrastructure in the recent past, the life expectancy has continuously increased in many countries. Therefore, it is very important to address the issues related to ageing society threatening to maintain the quality of life. The age-related hearing loss is a very important concern, among many others. According to World Health Organization (WHO), 'nearly 2.5 billion people are projected to have some degree of hearing loss and at least 700 million will require hearing rehabilitation' by 2050 [1]. Furthermore, over 1 billion young adults are at risk of developing hearing loss due to unsafe listening practices [1]. Hearing loss has very serious health consequences, including social isolation, depression, altered physical function, decreased activity engagement, lower quality

The associate editor coordinating the review of this manuscript and approving it for publication was Olutayo O. Oyerinde.

of life, greater cognitive decline, and an increased risk of dementia [2]. As a result, hearing aid users have showed cognitive deterioration comparable to older adults without hearing loss, making hearing aids an important tool that has been found to improve long-term cognition [3]. Therefore, it is very important to develop efficient modern digital hearing aid (DHAid) devices which will gain acceptability among all age groups [4], [5].

Hearing impairment is the partial or total loss of the hearing ability of an individual. In general, the use of DHAid devices may compensate this limitation, and hence, using DHAid devices may be essential for social integration of hearing impaired people in order to improve their auditory perception. Hearing aids were basically an analog item till the 1990s, when digital technology replaced completely the analog processing. This brings new features and functionality, impossible to be reached with the old technologies, viz., superior digital signal processing (DSP) capabilities for noise reduction and improved speech intelligibility, integration of active noise cancellation (ANC) to facilitate use in noisy situations, flexibility in fitting the instrument to the unique hearing loss characteristics of the consumer, implementation of efficient algorithms for feedback cancellation, directivity and source localization, frequency domain processing and better fitting to individual needs, and improved sound quality [6].

There are four common types of hearing aid models: in the canal (ITC), completely in the canal (CIC), in the ear (ITE), behind the ear (BTE) [7], where BTE DHAid device provides a greater flexibility for a somewhat large distance between the input microphone and the receiver loudspeaker. Yet, it cannot be completely tightly fitted to alleviate the problems related to the occlusion effect [8] which results in own voice being perceived as hollow. Additionally, a tight fitting may result is user complaining discomfort. For an open fitting, however, the unavoidable leakage path between the input microphone and receiver loudspeaker may lead to annoying feedback problems even at much lower gains compared to a closed fitting. A presence of such leakage path results in acoustic feedback, and the DHAid devices may suffer from oscillations, the phenomenon known as howling. The howling results in screeching or whistling sounds greatly annoying the user. In fact, howling is the major complaint for unacceptability of DHAid devices. Therefore, an integral part of contemporary DHAid devices is the acoustic feedback cancellation (AFC) technology, whose primary goal is to mitigate the acoustic feedback brought on by the DHAid's input microphone and loudspeaker's acoustic connection [9], [10], [11]. The improved performance feedback control algorithms are therefore indispensable for modern DHAid devices, where the aims are to provide 1) improved maximum stable gain (MSG), 2) good sound quality and low susceptibility to tonal signals at all gains avoiding very annoying entrainment artifacts [12], and last but not least, 3) fast tracking of possible variations in the feedback path.

Fig. 1 shows schematic and block diagrams for a typical DHAid device comprising single input microphone and a

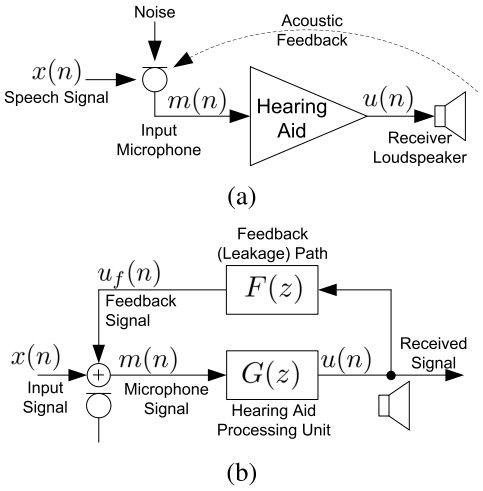

FIGURE 1. (a) A schematic diagram and (b) a block diagram of a typical digital hearing aid (DHAid) device.

single receiver loudspeaker. Essentially, DHAid acts as an amplifier to compensate for the hearing loss and to amplify the microphone signal $m(n)$ to give the amplified signal $u(n)$ to be played by the receive loudspeaker towards the user ear. Here $G(z)$ denotes the transfer function for the signal processing carried out by the DHAid. As stated earlier, due to open fitting that leakage path is unavoidable and acoustic feedback from receiver loudspeaker to the input microphone is always present. Thus, the microphone signal $m(n)$ comprises the desired/target signal $x(n)$ and undesired (but unavoidable) feedback signal $u_f(n)$. It is assumed that environmental noise is not present, which is typically the case when testing DHAid in a controlled laboratory settings. It is important to mention that noise reduction in DHAid devices is a separate research area and is not considered in this paper [13]. The measured acoustic feedback path, denoted as transfer function $F(z)$ in Fig. 1(b), comprises characteristics of digital to analog converter (DAC), the receiver loudspeaker, the physical leakage path between the receiver and the input microphone, the microphone itself, and analog to digital converter (ADC). The transfer function of the acoustic feedback path is subjected to variations due to the changes in the nearby acoustics, for example, due to the jaw movement of the user or when the user brings a smartphone near his/her ear.

Due to the time-varying nature of the system, the adaptive signal processing plays a pivotal role in designing adaptive AFC systems for practical DHAid devices. The efforts for developing efficient algorithms for AFC started back in 1990's when DHAid devices gained much attention [9], and the conventional AFC method is indeed based on the celebrated normalized least mean square (NLMS) algorithm [14]. The conventional NLMS-based AFC method is simple to implement, however, adaptive filter converging to a (suboptimal) biased solution poses a great threat. This biased convergence is due to the strong correlation present between the signals involved in the adaptive AFC filter's (NLMS-based) updated equation. A literature review shows that many solutions have been proposed: delay in the cancelation path [9] or

in the forward path [15], the prediction error method (PEM)-based AFC (PEM-AFC) [16], [17], [18], the probe signal-based AFC [19], [20], [21], frequency domain AFC [22], and two microphones-based method [23], [24], all aim at achieving an unbiased convergence.

One concept for the probe signal-based methods is a non-continuous adaptation (the so-called open-loop algorithm), in which the DHAid forward path is broken and a probe signal is injected at specific intervals, such as when howling is detected by an appropriate oscillation detector [19]. Three main characteristics should be considered in a howling detection algorithm: detect the howling in its initial stages before its high gain makes it intolerable for the user, to estimate the howling frequency component correctly, and above all, the detection algorithm should have low computational complexity [25]. However, the DHAid user experiences annoyance from the probe signal's ON/OFF switching. It has been investigated that the probe signal can be perceptually masked by using an adequate probe shaping filter [21]. Nevertheless, a constant presence of the probe signal requires either that the strength of the probe signal be low enough that would result in high signal-to-noise ratio (SNR) [20], or that a gain-controlled strategy may be developed and incorporated to automatically and gradually reduce (alongside the convergence of the AFC system) the strength of the probe signal [26], [27], [28].

The PEM-AFC makes the assumption that the target signal can be represented as an autoregressive (AR) process [16], [17], [18]. The inverse of such AR model can then be found and utilized to decorrelate the signals used in the AFC filter's adaptation. The PEM-based adaptive filtering with row operations (PEM-AFROW) [17], [29], the PEM-based partitioned-block frequency-domain (PEM-PBFD) adaptive filter [30], [31], and the PEM-based frequency domain Kalman filter (PEM-FDKF) algorithm [32] are just a few examples of the many versions for PEM-AFC implementation that can be found in the existing literature. A hybrid AFC algorithm has also been developed in [33] and [34] which selects between, depending upon the convergence condition of the AFC system, the classical NLMS update rule or PEM-based adaptation [16]. This decision is aided by a stability detector based on soft clipping. The main concept is to utilize fast convergence and low bias features of the standard NLMS and PEM-AFC, respectively [33].

We take into consideration a time-domain version of PEM-AFC in order to fairly compare it to the time-domain technique presented in this paper. The key question to answer is to do better in terms of implementation and real-time sample-by-sample processing, in contrast to compute the coefficients of decorrelation filter at regular intervals, for example, every 10 ms [27]. Essentially, a new method is proposed hereby which combines concepts of gain controlled probe-signal [27], lattice filtering-based AR modeling [35], and dual adaptive filtering [28]. The key features of the proposed method are summarized below:

1) *Dual adaptive filtering*: The proposed method comprises two adaptive filters operating in tandem.
2) *Lattice filtering-based decorrelation for the main adaptive AFC filter*: The main adaptive filter is excited by the DHAid receiver signal $u(n)$, which in a perfect world would be an amplified replica of the target signal $x(n)$. A lattice filtering-based pre-processing is utilized to produce the whitened reference signal that will be used in the associated NLMS-update equation for an unbiased adaptation of the main adaptive filter [36]. This effectively produces Newton-like adaptation and thus a fast convergence speed [35, Chapter 11].
3) *Probe signal-based adaptation of the auxiliary adaptive AFC filter*: A probe signal, uncorrelated with the target signal, serves as the 'input signal' and the error signal of the main adaptive AFC filter serves as the 'desired response' for the auxiliary adaptive AFC filter. The (uncorrelated) probe signal is combined with the received signal $u(n)$ along with a suitably selected delay. The auxiliary AFC filter shows an unbiased convergence as a result of the (uncorrelated) probe signal, but the DHAid user experiences it as an extremely irritating random noise. Therefore, as the AFC system converges, the level of the probe signal is (automatically) reduced. The low level excitation signal, on the other hand, slows convergence. Therefore, in order to speedup the slow convergence of the auxiliary AFC filter, a hybrid algorithm is suggested to perform the adaptation which combines gradient information from maximum Versoria criterion (MVC) [38] and delay-based NLMS [37].
4) *Controlling strength of probe signal*: A method of varying gain for the added probe signal has been employed: at startup, a large value is used for quick convergence, and as the system converges, the gain is decreased to a negligible value, resulting in a very high SNR at the steady-state.
5) *Coefficient transfer strategy*: Depending on the convergence condition of the two adaptive AFC filters, their coefficients are mutually exchanged. The idea is that both main and auxiliary adaptive AFC filters would converge to a reliable estimation of the true feedback path.

The rest of the paper is organized as follows. Section II gives a brief overview of PEM-AFC in connection with NLMS-based traditional method. Sections III describes the proposed method as outlined above, and Section IV presents results of computer simulations. Finally, conclusion is given in Section V. A short version of this paper was presented at a conference [39].

II. OVERVIEW OF CLASSICAL APPROACHES FOR AFC

A. CONVENTIONAL LMS/NLMS ADAPTIVE FILTERING

A block diagram for the traditional AFC technique employing the NLMS algorithm is shown in Fig. 2. It is assumed that

the feedback (leakage) path $F(z)$ is a finite impulse response (FIR) filter having L coefficients. The microphone signal $m(n)$ is a mixture of the input signal $x(n)$ and the acoustic feedback signal $u_f(n)$, and can be expressed as

$$m(n) = x(n) + u_f(n), \tag{1}$$

where $u_f(n)$ can be expressed as

$$u_h(n) = f(n) * u(n) = \boldsymbol{u}^T(n)\boldsymbol{f}, \tag{2}$$

where $f(n) \overset{z}{\longleftrightarrow} F(z)$ denotes impulse response of $F(z)$, $*$ denotes convolution, $\boldsymbol{f} = [f_0, f_1, \cdots, f_{L-1}]^T$ is the coefficient vector for the $F(z)$ (assumed to be a linear time-invariant (LTI) system for discussion presented in this Section), and $\boldsymbol{u}(n) = [u(n), u(n-1), \cdots, u(n-L+1)]^T$ is the received signal vector. In Fig. 2, $H(z)$ is the adaptive AFC filter aimed to perform neutralization of the feedback component $u_f(n)$ present in the microphone signal. The AFC filter $H(z)$ is also assumed to be an FIR filter of length L and is excited by the receiver loudspeaker signal $u(n)$. Therefore, the output signal of AFC filter $H(z)$, $y_h(n)$, can be expressed as

$$y_h(n) = h(n) * u(n) = \boldsymbol{u}^T(n)\boldsymbol{h}(n), \tag{3}$$

where $h(n) \overset{z}{\longleftrightarrow} H(z)$ denotes impulse response of $H(z)$, and $\boldsymbol{h}(n) = [h_0(n), h_1(n), \cdots, h_{L-1}(n)]^T$ is the coefficient vector for the AFC filter $H(z)$. The output signal $y_h(n)$ of the AFC filter $H(z)$ is compared with the microphone signal $m(n)$ to compute the 'error' signal $e_h(n)$ as

$$\begin{aligned} e_h(n) &= m(n) - y_h(n), \\ &= x(n) + u_f(n) - y_h(n), \\ &= x(n) + \boldsymbol{u}^T(n)\left[\boldsymbol{f} - \boldsymbol{h}(n)\right]. \end{aligned} \tag{4}$$

The NLMS algorithm updates the coefficients of adaptive AFC filter $H(z)$ [14] as

$$\boldsymbol{h}(n+1) = \boldsymbol{h}(n) + \frac{\mu}{\|\boldsymbol{u}(n)\|^2 + \delta} e_h(n)\boldsymbol{u}(n), \tag{5}$$

where $\|\cdot\|$ is the Euclidean norm of the quantity inside, μ is the fixed step-size (FSS) parameter, and δ is small positive constant used as a regularization parameter. Ideally speaking, the AFC adaptive filter $H(z)$ is trying to identify the feedback path $F(z)$ as $\boldsymbol{h}(n) \to \boldsymbol{f}$ as $n \to \infty$ resulting in $e_h(n) \to x(n)$, and hence the DHAid input signal $s(n)$ is derived as $s(n) \equiv e_h(n)$. Due to a strong correlation between $m(n)$ (used as a 'desired' response for $H(z)$) and $u(n)$ (used as input to $H(z)$), regrettably, $H(z)$ converges to a (suboptimal) biased solution [40], [41]:

$$\boldsymbol{h}(n) \to \boldsymbol{f} + \boldsymbol{R}_{\boldsymbol{uu}}^{-1}\boldsymbol{r}_{\boldsymbol{u}x}, \tag{6}$$

where the second term on the right-hand-side (RHS) is the biasing term, and its presence shows that $\boldsymbol{h}(n)$ may not converge to the desired solution $\boldsymbol{f}$. As shown in (6), the biasing term comprises product of inverse of the auto-correlation matrix $\boldsymbol{R}_{\boldsymbol{uu}} = E\left\{\boldsymbol{u}(n)\boldsymbol{u}^T(n)\right\}$ of receiver (loudspeaker) signal $u(n)$, and the cross-correlation vector $\boldsymbol{r}_{\boldsymbol{u}x} = E\left\{\boldsymbol{u}(n)x(n)\right\}$ between $u(n)$ and the input signal $x(n)$. The resulting effect

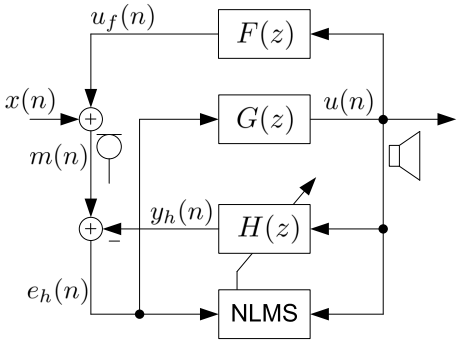

FIGURE 2. Classical NLMS algorithm-based method for AFC in DHAid devices.

in AFC is twofold: first, the adaptive filter estimates and cancels only part of the feedback signal $u_f(n)$; second, it also estimates and cancels part of the system input signal $x(n)$. As a consequence, the feedback-compensated signal $s(n) \equiv e_h(n)$ is a distorted estimate of the target signal $x(n)$ [42]. As a result, the method in Fig. 2 cannot be applied in a continuous adaptation mode; rather, the adaptation must be ceased after an 'acceptable' convergence has been reached. Nevertheless, the key property of the conventional NLMS-based AFC is it fast convergence speed, thanks to AFC adaptive filter being excited by a strong signal $u(n)$ which is essentially expected to be an amplified version of $x(n)$.

B. CLASSICAL PEM-AFC AND ITS VARIANTS

It is straightforward to comprehend from (6) that the biasing term can be reduced, if cross-correlation between $u(n)$ and $x(n)$ can be reduced. The pre-whitening filter $B(z)$ is used by PEM-AFC utilizing NLMS algorithm (see Fig. 3) to enhance NLMS algorithm convergence. The AR modeling from the DHAid input signal $s(n) = e_h(n)$ is performed using the Levinson-Durbin algorithm [43] to generate the coefficients $\boldsymbol{b}(n) = [1, b_1(n), b_2(n), \cdots, b_{L_p}(n)]^T$ of $B(z)$. Here, Lp is the order of $B(z)$. After obtaining the pre-filtered signals $e'_h(n)$ and $u'(n)$ using the coefficients of $B(z)$, the coefficients of AFC filter $H(z)$ are updated using NLMS algorithm as

$$\boldsymbol{h}(n+1) = \boldsymbol{h}(n) + \frac{\mu}{\|\boldsymbol{u}'(n)\|^2 + \delta} e'_h(n)\boldsymbol{u}'(n). \tag{7}$$

It has been demonstrated that PEM-AFC significantly resolves the biased convergence issue of the traditional NLMS-based AFC method [16]. A literature review shows that many variants have been proposed to improve upon the performance of PEM-AFC method [16], [17], [18], [29], [30], [31], [32], [33], [34]. Considering that the conventional NLMS-based AFC provides fast re-convergence from a howling period, while the PEM-AFC algorithm addresses the biasing problem, a very interesting idea of a hybrid method merging the best properties of both approaches, have been proposed in [33]. This method is based on a hybrid switched combination of two approaches. A properly designed stability detector has been developed to detect whether the error signal

after the feedback canceler is outside a certain bound, indicating instability. When instability is detected, the conventional NLMS-based AFC algorithm is used to achieve fast convergence, whereas otherwise the PEM-AFC is employed owing to its low bias properties [33].

In this contribution, we address the fundamental issue of updating the decorrelation filter $B(z)$ on the bases of AR-modeling techniques. As discussed in [18], for the classical method shown in Fig. 3 (and in fact for other variants too), the AR model of order $Lp = 10 - 20$ can be updated every $10 - 20$ ms for a speech signal at a sampling frequency $F_s = 16$ kHz. The question we ask: Can we do better to perform continuous decorrelation along with continuous adaptation of AFC filter(s)? This question is very important, especially given that when the DHAid is in operation, the target signal characteristics may switch between speech, audio (music, TV, etc.), telephone ring, fire alarm, etc. As a result, performing the decorrelation constantly on a sample-by-sample basis would be ideal. This is exactly what this study explores.

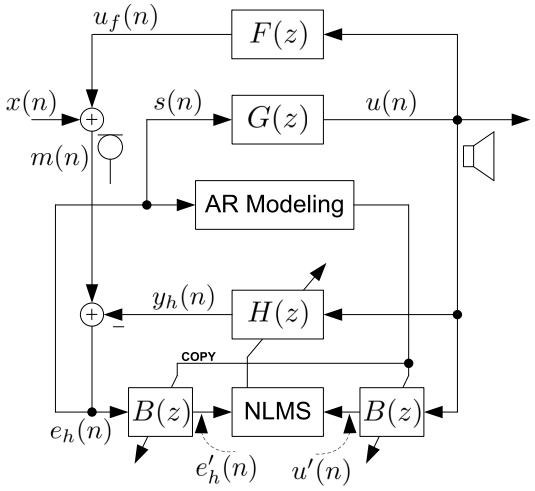

FIGURE 3. Prediction error method (PEM)-based method for unbiased AFC in DHAid devices.

III. PROPOSED METHOD

A. IMPLEMENTATION STRUCTURE

The implementation structure for the proposed method is adopted from a previous work presented in [44]. As shown in Fig. 4, the AFC in the previous approach has been achieved by two adaptive filters, $H(z)$ and $V(z)$, working in tandem. The main adaptive AFC filter $H(z)$ is excited by the receiver loudspeaker signal $u(n)$ (as in conventional AFC approach shown in Fig. 2), and it is tasked with mitigating the effect of the feedback component $u_f(n)$. The auxiliary adaptive filter $V(z)$ is excited by the internally generated probe signal $p(n)$, and is expected to provide neutralization for the feedback component $p_f(n)$ due to the probe signal $p(n)$. The microphone signal is now given as

$$m(n) = x(n) + \left[u_f(n) + p_f(n)\right], \tag{8}$$

where $p_f(n) = f(n) * p(n - D)$ is the acoustic feedback component due to the delayed probe signal $p(n - D)$ where D is an appropriately selected delay as explained later. The expression for the error signal $e_h(n)$ for the main adaptive AFC filter $H(z)$ is given as

$$e_h(n) = x(n) + \left[u_f(n) - y_h(n)\right] + p_f(n), \tag{9}$$

where grouping of $u_f(n)$ and $y_h(n)$ signifies that output signal $y_h(n)$ from $H(z)$ is expected to 'take care' of $u_f(n)$. Using error signal $e_h(n)$ of main adaptive AFC filter $H(z)$ as a desired response for the auxiliary adaptive AFC filter $V(z)$, the error signal for $V(z)$, $e_v(n)$, is given as

$$e_h(n) = x(n) + \left[u_f(n) - y_h(n)\right] + \left[p_f(n) - y_v(n)\right], \tag{10}$$

where the second bracketed term on the RHS signifies that output $y_v(n)$ from the auxiliary AFC filter $V(z)$ is expected to reduce the feedback component $p_f(n)$. Without going into details [44], a few remarks for this method are as follows:

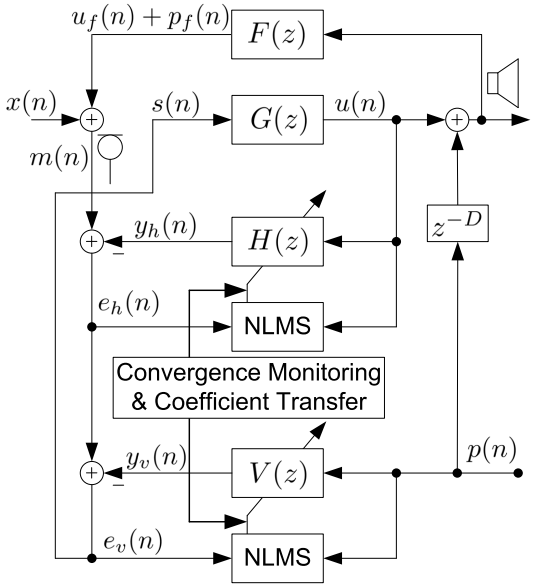

FIGURE 4. Block diagram for a previous method for continuous AFC in DHAid devices.

- The main AFC filter $H(z)$ is excited by $u(n)$ which is an amplified version of (ideally) $x(n)$, and hence convergence of $H(z)$ is very fast; however, it may converge to a biased solution as discussed earlier.
- It is assumed that $p(n)$ is a low-level white signal and is uncorrelated with the input signal $x(n)$ and hence with the receiver signal $u(n)$.
- The auxiliary AFC filter $V(z)$, though converging slowly being excited by a low-level probe signal $p(n)$, would give a good steady-state estimate of the acoustic feedback path $F(z)$.
- The delay D increases the effective length of 'plant' to be identified by the auxiliary adaptive AFC filter $V(z)$. Therefore, $V(z)$ is an extended-length filter with initial

coefficients converging to zero (to model the appended delay D), and the rest of coefficient model the feedback path $F(z)$.
- The appended delay D and the corresponding initial coefficients of $V(z)$ (modeling the delay) help in designing a convergence monitoring and coefficients strategy.
- The coefficient transfer strategy is designed such that the biased convergence of $H(z)$ is reduced (if not competently avoided) and the initial convergence of $V(z)$ must be improved. This ensures that both $H(z)$ and $V(z)$ give good estimate of $F(z)$; hence, $H(z)$ takes care of $u_f(n)$, and $V(z)$ takes care of $p_f(n)$ resulting in $e_v(n) \rightarrow x(n)$ and thus, $s(n) \equiv e_v(n)$ can be used as an input to the DHAid processing unit $G(z)$ for amplification and further (user-specific) processing.

Our experiments have shown that previous method cannot fully mitigate the biased convergence issue of the first AFC filter $H(z)$. Furthermore, the low-level probe signal $p(n)$ results in sluggish convergence of auxiliary AFC filter $V(z)$. Another important issue is presence of the probe signal during all operating condition of the DHAid device. Though a low level signal, $p(n)$ is not completely absent and may appear as a background hissing sound which is not at all acceptable for the practical DHAid devices. The proposed method presented in this paper, addresses all these issues as well as responds to the question raised earlier, and is explained below.

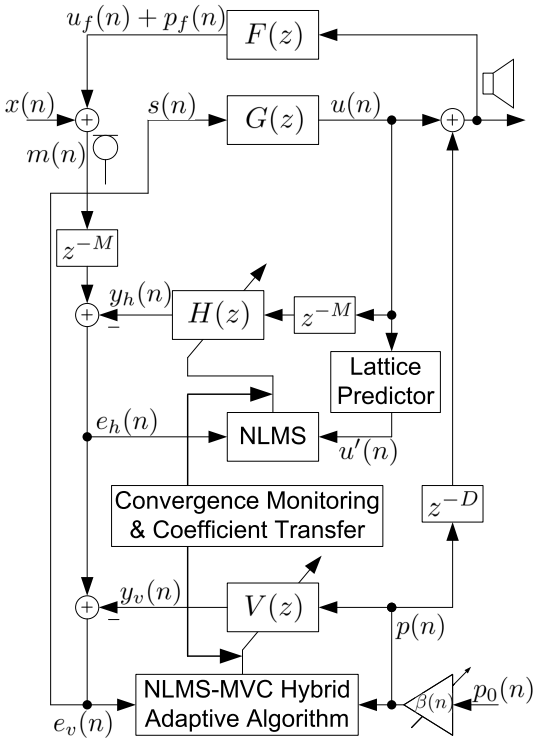

FIGURE 5. Block diagram for the proposed method for continuous unbiased AFC in DHAid devices.

B. LATTICE FILTERING-BASED ADAPTATION OF THE MAIN AFC FILTER H(z)

As shown in Fig. 5, the proposed method for AFC in DHAid devices essentially builds upon the previous approach described earlier (see Fig. 4), and is based on dual adaptive filters operating in tandem. Here, the delay D is carefully chosen to be employed in the technique (explained later) that will be used to track the convergence of the auxiliary AFC filter $V(z)$. In order to facilitate the lattice prediction-based decorrelation [35], a delay M is used with the desired response as well as input of $H(z)$. As a rule of thumb, the delay M is chosen in line with the order of the lattice backward prediction-error filter that is used to accomplish whitening/decorrelation of $u(n)$ prior to being employed in the update equation of $H(z)$.

The desired response for adapting $H(z)$ is taken from the microphone signal $m(n)$. Accordingly, the error signal $e_h(n)$ is calculated as

$$e_h(n) = m(n-M) - y_h(n), \tag{11}$$

where $y_h(n)$ is the output signal of the AFC filter $H(z)$ expressed as

$$y_h(n) = \boldsymbol{h}^T(n)\boldsymbol{u}(n-M), \tag{12}$$

where $\boldsymbol{u}(n-M) = [u(n-M), u(n-M-1), \cdots, u(n-M-L+1)]^T$ is vector for the (M-sample) delayed received signal $u(n-M)$. The NLMS algorithm, to update the coefficients of the main AFC filter $H(z)$, is given as

$$\boldsymbol{h}(n+1) = \boldsymbol{h}(n) + \frac{\mu_h}{\|\boldsymbol{u}'(n)\|^2 + \delta} e_h(n)\boldsymbol{u}'(n), \tag{13}$$

where $\boldsymbol{u}'(n) = [u'(n), u'(n-1), \cdots, u'(n-L+1)]^T$ is the whitened or decorrelated signal vector, and μ_h is a fixed-valued step-size parameter. The whitened signal $u'(n)$ is computed via lattice prediction-based filtering, as explained below. The details for block 'lattice predictor' (taking $u(n)$ as an input and generating the decorrelated signal $u'(n)$) is shown in Fig. 6, and corresponding algorithms are summarized in Table 1 and 2 [35].

Table 1 provides the details of lattice predictor algorithm [35, Chapter 11], which is employed to compute M-th order lattice predictor's parameters. These parameters are forward prediction errors, backward prediction errors, and reflection coefficients, and are denoted by the variables $f_m(n)$, $b_m(n)$ and $k_m(n)$ ($m = 1, 2, \cdots, M$), respectively. The step-size parameter for adjusting the reflection coefficients is μ_k, and λ is the forgetting factor which is selected in the range $(0.9 < \lambda < 1)$. It is well known that the stability of lattice-structure-based filters is guaranteed if and only if the reflections coefficients $k_m(n)$ stay less than unity in magnitude [43]. Therefore, the role of the parameter γ (a positive constant) is to prevent the reflection coefficients $k_m(n)$ from diverging. Table 2 shows the algorithm which takes the estimates from algorithm in Table 1, and produces samples of whitened signal vector $\boldsymbol{u}'(n)$

It can be seen from a comparison of (5) and (13) that the latter uses $\boldsymbol{u}'(n)$ (instead of $\boldsymbol{u}(n)$) in the update equation of the NLMS algorithm. It is important to note that this produces an algorithm similar to the NLMS-Newton, which considerably improves convergence. The reader is directed to [35, Chapter 11] for more information on the algorithm's convergence analysis.

C. HYBRID ADAPTIVE ALGORITHM FOR THE AUXILIARY AFC FILTER $V(z)$

The probe signal $p(n)$ excites the auxiliary adaptive AFC filter $V(z)$, as shown in Fig. 5. The receiver signal $u(n)$ is combined with the probe signal after being delayed by D samples. Due to the presence of the inserted delay z^{-D}, the AFC filter $V(z)$ has a task of identifying an overall cascade system of feedback path and the delay z^{-D}. Consequently, the auxiliary AFC filter $V(z)$ is an FIR filter having (extended) length $D+L+1$, with its coefficient vector being given as

$$\boldsymbol{w}(n) = \begin{bmatrix} \boldsymbol{w}_{\mathrm{D}}(n) \\ \boldsymbol{w}_{\mathrm{F}}(n) \end{bmatrix} = \begin{bmatrix} v_0(n) \\ \vdots \\ v_D(n) \\ v_{D+1}(n) \\ \vdots \\ v_{D+L}(n) \end{bmatrix}_{(D+L+1)\times 1}, \quad (14)$$

where the initial part $\boldsymbol{v}_D(n) = [v_0(n), v_1(n), \cdots, v_{D-1}(n), v_D(n)]^T$ makes an attempt to model the introduced delay z^{-D}, and the latter coefficients $\boldsymbol{v}_F(n) = [v_{D+1}(n), \cdots, v_{D+L}(n)]^T$ provide an estimate for the feedback path's coefficients. The error signal $e_h(n)$ from the main AFC filter $H(z)$ acts as a 'desired' response for the auxiliary AFC filter $V(z)$ to give the corresponding error signal $e_v(n)$ as

$$e_v(n) = e_h(n) - y_v(n), \quad (15)$$

where $y_v(n)$ denotes the output signal of the auxiliary AFC filter $V(z)$, and is computed as

$$y_v(n) = \boldsymbol{v}^T(n)\boldsymbol{p}(n), \quad (16)$$

where $\boldsymbol{p}(n)$ is the input signal vector for the extended-length AFC filter $V(z)$ and can be expressed as

$$\boldsymbol{p}(n) = \begin{bmatrix} \boldsymbol{p}_{\mathrm{D}}(n) \\ \boldsymbol{p}_{\mathrm{F}}(n) \end{bmatrix} = \begin{bmatrix} p(n) \\ p(n-1) \\ \vdots \\ p(n-D-L) \end{bmatrix}_{(D+L+1)\times 1}, \quad (17)$$

where sample of $p(n)$ are obtained from the probe signal $p_0(n)$ via the time-varying gain $\beta(n)$. The computation of $\beta(n)$ is detailed later; however, the main concept is to lower the probe signal intensity as the AFC system converges. As a result, the SNR at the DHAid output would be improved, though the AFC filter $V(z)$ would become slow. It has been reported that MVC-based adaptive filtering exhibits robust performance for non-Gaussian signals [38], which are indeed encountered in the DHAid devices. Therefore, it is suggested to use the following hybrid adaptive technique to get a fast convergence speed for $V(z)$:

$$\boldsymbol{v}(n+1) = \boldsymbol{v}(n) + \mu_v(n)\Delta\boldsymbol{V}_{\mathrm{NLMS}}(n) + \tilde{\mu}_v\Delta\boldsymbol{V}_{\mathrm{MVC}}(n), \quad (18)$$

where $\Delta\boldsymbol{V}_{\mathrm{NLMS}}(n)$ corresponds to the gradient information as in the classical NLMS algorithm as

$$\Delta\boldsymbol{V}_{\mathrm{NLMS}}(n) = \frac{e_v(n)\boldsymbol{p}(n)}{\|\boldsymbol{p}(n)\|_2^2 + \delta}, \quad (19)$$

and where $\mu_v(n)$ is a time varying step-size parameters computed using delay-based technique as [37]

$$P_{e_v}(n) = \lambda P_{e_v}(n-1) + (1-\lambda)e_v^2(n), \quad (20)$$

$$\hat{N}_{\mathrm{D}}(n) = \lambda\hat{N}_{\mathrm{D}}(n-1) + (1-\lambda)\left(\|\boldsymbol{w}_{\mathrm{D}}(n)\|^2\|\boldsymbol{v}_{\mathrm{D}}(n)\|^2\right)/D, \quad (21)$$

$$\mu_v(n) = \lfloor \frac{C_1\hat{N}_{\mathrm{D}}(n)}{P_{e_v}(n)+\delta} \rfloor_{\mu_{v_{\min}}}, \quad (22)$$

where C_1 signifies an empirical constant, $P_{e_v}(n)$ stands for an estimate of the power of $e_v(n)$, and $\mu_{v_{\min}}$ is the minimum

TABLE 1. Summary of algorithm to compute parameters of the M-th order lattice predictor.

Parameters: λ, μ_k, δ, γ.
Available from the previous iteration:
$k_1(n-1), k_2(n-1), \cdots, k_M(n-1)$;
$P_0(n-1), P_1(n-1), \cdots, P_M(n-1); b_0(n-1)$;
Available from the hearing aid loudspeaker: $u(n)$
To compute: $b_1(n), b_2(n), \cdots, b_M(n)$;
$k_1(n), k_2(n), \cdots, k_M(n)$;
$P_0(n), P_1(n), \cdots, P_M(n)$;

$f_0(n) = b_0(n) = u(n)$
$P_0(n) = \lambda P_0(n-1) + (1-\lambda)\dfrac{(f_0^2(n) + b_0^2(n-1))}{2}$
for $m = 1 : M$
$f_m(n) = f_{m-1}(n) - k_m(n)b_{m-1}(n-1)$
$b_m(n) = b_{m-1}(n-1) - k_m(n)f_{m-1}(n)$
$k_m(n) = k_m(n-1) +$
$\dfrac{\mu_k}{P_{m-1}(n)+\delta}(f_{m-1}(n)b_m(n) + b_{m-1}(n-1)f_m(n))$
$P_m(n) = \lambda P_m(n-1) + (1-\lambda)\dfrac{(f_m^2(n) + b_m^2(n-1))}{2}$
if $|k_m(n)| > \gamma, \quad k_m(n) = \gamma \cdot \mathrm{sgn}(k_m(n)),$ **end if**
end for

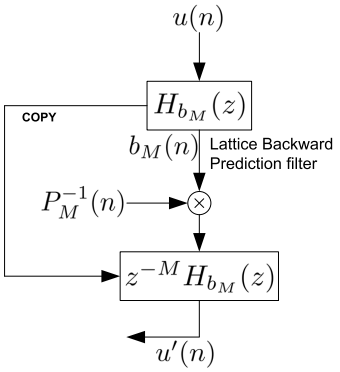

FIGURE 6. Lattice-backward prediction-filter based method to generate the (de-correlated) input signal $u'(n)$ for the update equation of the main adaptive filter $H(z)$ in the proposed method shown in Fig. 5.

value for the step-size $\mu_v(n)$ [27]. Here, $\lfloor\cdot\rfloor_{\mu_{2_{\min}}}$ denotes the `floor` operation, i.e., if $\mu_v(n) \leq \mu_{v_{\min}}$ then $\mu_v(n) = \mu_{v_{\min}}$.

In (18), the contribution of the increment vector $\Delta\boldsymbol{V}_{\text{MVC}}(n)$ is controlled via experimentally chosen fixed step-size parameter $\tilde{\mu}_v$, and to compute $\Delta\boldsymbol{V}_{\text{MVC}}(n)$, the following MVC-based adaptive method is employed [28], [38]:

$$\{e_v(n)\} = \{|e_v(n)|, |e_v(n-1)|, \cdots, |e_v(n-N_w+1)|\}, \tag{23}$$

$$\overline{e_v}(n) = \lambda\overline{e_v}(n-1) + (1-\lambda)\min\{e_v(n)\}, \tag{24}$$

$$\theta = \lceil C_2\overline{e_v}(n)\rceil^{C_2}; \quad \tau = 1/(2\theta)^q, \tag{25}$$

$$\Delta\boldsymbol{V}_{\text{MVC}}(n) = \frac{\text{sgn}\{e_v(n)\}|e_v(n)|^{q-1}\boldsymbol{v}(n)}{\left[1+\tau|e_v(n)|^q\right]^2}, \tag{26}$$

where $\{e_v(n)\}$ is collection/window of N_w recent values of $e_v(n)$, q is a fractional number to account for the non-Gaussian nature of signals, and $\lceil\cdot\rceil^{C_2}$ denotes the `ceil` operation, i.e., if $\theta \geq C_2$ then $\theta = C_2$ where C_2 is another empirical constant. Finally, the error signal $e_v(n)$ (15) used in adaptation of the auxiliary AFC filter $V(z)$ is input to the DHAid processing unit $G(z)$, i.e., $s(n) \equiv e_v(n)$.

Let's now clarify how the probe signal, $p(n)$, is produced in order to activate the AFC filter, $V(z)$? As previously mentioned, there are two components to the coefficients of $V(z)$: $\boldsymbol{v}_{\text{D}}(n)$ and $\boldsymbol{v}_{\text{F}}(n)$. Assume that all of the initial coefficients (i.e. vector $\boldsymbol{v}_{\text{D}}(n)$) are initialized to 1. These coefficients aim to model the added delay z^{-D}, and hence, are anticipated to converge to a pure delay as

$$\begin{aligned}\boldsymbol{v}_{\text{D}}(n) &= [v_0(n), v_1(n), \cdots, v_{D-1}(n), v_D(n)]^T \\ &\to [0, 0, \cdots, 0, 1]^T.\end{aligned} \tag{27}$$

As a result, the required solution for $\boldsymbol{v}_{\text{D}}(n)$ is known a priori, and this knowledge may be utilized to check on the convergence of the AFC filter $V(z)$. We basically define a parameter.

$$\alpha(n) = \frac{1}{D}\sum_{j=0}^{D-1}|v_j(n)|^2. \tag{28}$$

The behavior of $\alpha(n)$ can be understood pretty simply. The initial value is $\alpha(0) = 1$ (as $\boldsymbol{v}_{\text{D}}(n)$ has been initialized as a unity vector). As $V(z)$ converges, the coefficients $v_0(n), v_1(n), \cdots, v_{D-1}(n)$ are expected to converge to zero (see (27)), and hence the parameter $\alpha(n)$ converges to a tiny value (ideally close to zero). This insight leads us to calculate the time-varying gain $\beta(n)$ as

$$\beta(n) = \lceil\alpha(n)\rceil^1 \tag{29}$$

which is restricted to the maximum value of 1 so that gain does not become excessively large in some situations of divergence, for example, when the characteristics of acoustic path suddenly change during the DHAid is in use. Finally, the gain parameter $\beta(n)$ is used to regulate the probe signal as

$$p(n) = \beta(n)p_0(n), \tag{30}$$

where $p_0(n)$ denotes a white zero-mean random Gaussian signal. When $\alpha(n)$ is close to unity (see (29)), which denotes that $V(z)$ is not yet convergent, and thus $p(n) \approx p_0(n)$. Alongside the convergence of the auxiliary AFC adaptive filter $V(z)$, the parameters $\alpha(n)$ and $\beta(n)$ become very small (ideally close to zero). Therefore, the probe signal $p(n)$ is tuned to a negligible value as the auxiliary AFC filter $V(z)$ converges.

TABLE 2. Summary of algorithm to compute the samples of the decorrelated signal $u'(n)$ for adaptive algorithm of the main AFC filter $H(z)$ in the proposed method.

Inputs: $b_M(n); k_1(n), k_2(n), \cdots, k_M(n); P_M(n)$
To do: Update $\boldsymbol{u}'(n) = [u'(n), u'(n-1), \cdots, u'(n-L+1)]^T$;
$u_a(n-j) = u_a(n-j+1); j = L-1, L-2, \cdots, 1$
$f'_0(n) = b'_0(n) = b_M(n);$
for $m = 1 : M$
$\quad f'_m(n) = f'_{m-1}(n) - k_m(n)b'_{m-1}(n-1);$
$\quad b'_m(n) = b'_{m-1}(n-1) - k_m(n)f'_{m-1}(n);$
end for
$u'(n) = \dfrac{f'_M(n)}{(P_M(n)+\delta)};$

D. CONVERGENCE MONITORING & COEFFICIENT TRANSFER

Let's see how the appended delay z^{-D} helps in designing an efficient strategy for convergence monitoring and coefficient transfer. The key idea is to inspect the convergence of two adaptive AFC filters such that 1) their coefficients are mutually transferred to help aid each other in achieving a reliable estimate of the true acoustic feedback path $F(z)$, 2) the probe signal gain $\beta(n)$ is reduced at the steady-state, and 3) sudden change in the path is automatically detected to increase the strength of the probe signal for fast re-convergence of the AFC system.

The receiver (loudspeaker) signal $u(n)$, which is expected to be (ideally) an amplified version of the target signal $x(n)$, excites the AFC filter $H(z)$ in the proposed technique (see Fig. 5). Being excited by a large level signal, $H(z)$ converges quickly, yielding $P_{e_h}(n) < P_{e_v}(n)$, where $P_{e_h}(n)$ signifies an estimate of the power of $e_h(n)$ that may be calculated using a lowpass estimator as given in (20). The coefficients of main AFC filter $H(z)$ are copied to $\boldsymbol{v}_{\text{F}}(n)$ (part of the auxiliary AFC filter $V(z)$ expected to identify $F(z)$) at the start-up.

As soon as parameter $\alpha(n)$ drops below a certain threshold i.e., $\alpha(n) < T_1$, it is expected that the auxiliary AFC filter $V(z)$ has converged. From continuous exchange of both filters' coefficients, it is safe to assume that the main AFC filter $H(z)$ has converged too, and an estimate of the true acoustic feedback path $F(z)$ can be obtained from the main AFC filter $H(z)$ as $\widetilde{\boldsymbol{f}}(n) = \boldsymbol{h}(n)$. Considering the nature of the parameter $\alpha(n)$ as described in (28), the threshold T_1 may be chosen as a small number near to zero. Further adaption of $H(z)$ is ceased because a reliable estimate of $F(z)$ has already been acquired. On the other hand, the auxiliary adaptive AFC filter $V(z)$ is continuously adapted to track potential fluctuations of $F(z)$. The procedure to track variations in $F(z)$ is as follows.

The *misalignment* being calculated as the normalized squared deviation (NSD) for the auxiliary adaptive AFC filter

$V(z)$ can be computed using the estimate $\widetilde{\boldsymbol{f}}(n)$, as

$$\mathrm{NSD}_v(n) = 10\log\left\{\frac{\|\widetilde{\boldsymbol{f}}(n) - \boldsymbol{v}_{\mathrm{F}}(n)\|^2}{\|\widetilde{\boldsymbol{f}}(n)\|^2}\right\}. \tag{31}$$

The three parameters $\alpha(n)$, $\mathrm{NSD}_v(n)$, and $P_{e_v}(n)$ (power of the error signal $e_v(n)$), may now be used to examine the convergence state of the auxiliary AFC filter $V(z)$. It's easy to comprehend and select appropriate thresholds for these three factors, as $\alpha(n)$ should be 'small', $\mathrm{NSD}_v(n)$ should be negative, and $P_{e_v}(n)$ should be small for a converged/coverging $V(z)$. If, for instance, $\alpha(n) > 1$, $\mathrm{NSD}_v(n) > T_2$, and $P_{e_v}(n)$ also increase, then the AFC filter $V(z)$ has diverged, suggesting that the unknown feedback path $F(z)$ must has been altered. Re-initializing $H(z)$ and $V(z)$ and resuming the adaptation of $H(z)$ allow for the estimation of modified $F(z)$.

IV. COMPUTER SIMULATIONS

A. SIMULATION PARAMETERS

This section presents results of extensive numerical simulations carried out to understand the performance of the proposed method in comparison with the key related art. It is customary to consider a gain-delay model for the DHAid processing unit $G(z)$, and this work is no exception. Essentially, the DHAid device processing unit is modeled as $G(z) = Kz^{-\Delta}$, where Δ denotes the permitted delay for necessary processing and K denotes the gain factor for the desired amplification. In this study, the numerical experiments have been performed for two gain settings of $K = 10$ and $K = 20$, and the processing delay has been fixed to $\Delta = 40$ samples (2.5 ms for the adopted sampling frequency of 16 kHz). A small delay of 2.5 ms has been selected for reasons remarked earlier for the delay requirements in modern DHAid which are becoming almost delay-less devices.

It is important to mention that each method (considered in this simulation study) employs a different strategy to deal with the issues of the conventional NLMS AFC. Therefore, the corresponding parameters in various situations have been experimentally adjusted with the objective of fast and stable convergence of the respective method. The methods included in this simulation study (and corresponding simulation parameters) are as follows:

1) Conventional NLMS AFC: The NLMS algorithm-based conventional AFC method as shown in Fig. 1. ($\mu = 1 \times 10^{-3}$, $\delta = 1 \times 10^{-4}$.)
2) Probe-shaping AFC [21]: A probe signal-based method where a probe shaping filter is introduced to perceptually mask the probe signal (not discussed in this paper and reader is referred to [21] and [27] for further details). ($\mu = 1 \times 10^{-3}$, $\delta = 1 \times 10^{-4}$, $\mathrm{SNR}_{\mathrm{probe}} = \sigma_p^2/\sigma_x^2 = -20$ dB.)
3) PEM-AFC [16]: A time-domain implementation of PEM-AFC as shown in Fig. 3. The decorrelation prefilter $B(z)$ is of order $Lp = 16$, and AR modeling-based prediction algorithm is used to update its coefficients every 10 ms [27]. ($\mu = 1 \times 10^{-3}$ ($K = 10$), $\mu = 5 \times 10^{-4}$ ($K = 20$) $\delta = 1 \times 10^{-4}$.)
4) Basic Method [44]: The proposed method builds upon the previous method shown in Fig. 4, therefore, the previous method is treated as a 'basic method' for the performance comparison. ($\mu_h = 1 \times 10^{-3}$, $\delta = 0.02$, $\lambda = 0.97$, $\mathrm{SNR}_{\mathrm{probe}} = \sigma_v^2/\sigma_s^2 = -15$ dB, $D = 64$, $\mu_{v_{\min}} = 1 \times 10^{-6}$, $T_1 = 1 \times 10^{-3}$, $T_2 = -20$ dB.)
5) Proposed Method-a: A version of proposed method (in Fig. 5) by considering only NLMS-adaptive algorithm instead of NLMS-MVC hybrid adaptive algorithm for the auxiliary AFC filter $V(z)$. The objective is to understand if the hybrid adaptive filtering does really provide any performance again [36]. ($\mu_h = 1 \times 10^{-4}$, $\delta = 0.02$, $\lambda = 0.97$, $D = 64$, $\mu_k = 1 \times 10^{-6}$, $\gamma = 0.9$, $M = 32$, $\mu_{v_{\min}} = 1 \times 10^{-6}$, $C_1 = 1$, $T_1 = 1 \times 10^{-3}$, $T_2 = 10$ dB, $p_0(n)$ is zero-mean unit-variance white Gaussian noise.)
6) Proposed Method-b: The proposed method as fully described in this paper (see Fig. 5) (with preliminary results presented at a conference [39]). ($\mu_h = 5 \times 10^{-4}$ ($K = 10$), $\mu_h = 2.5 \times 10^{-4}$ ($K = 20$), $\tilde{\mu}_v = 7.5 \times 10^{-3}$, $C_1 = 0.097$, $C_2 = 0.97$, $q = 1.75$, $N_w = 8$, $p_0(n)$ and rest of parameters are same as listed therein for the Proposed-a method.)

Another previous work [27] and [28] considers appending delay in the forward path of the DHAid device, after the probe signal $p(n)$ has been mixed with receiver signal $u(n)$. This results in requiring to use extended-length coefficients vectors for both main and auxiliary AFC filters. The delay in the forward path appears in series with the DHAid processing unit $G(z)$, and hence, would limit the delay available for processing in $G(z)$. Such an appended delay in the forward path may be prohibited for practical DHAid devices, as it may severely affect the 'stereo' listening experience; especially if the DHAid device is needed only for one ear. In such a case, a delayed signal in one ear using DHAid would interact with a non-delayed signal from the normal ear. This may severely perturb the stereo perception and quality of listening experience. Additionally, such a delay in the forward path may cause problems with the listening experience for binaural DHAid devices too, for example, when the user is watching TV [46]. In this case, the visual signal is the relatively less-delayed reference, and the user may experience audio-video dyssynchrony resulting in the lip movements not matching with the sounds that follow. It has been reported that disruptions in audio-visual integration such as these occur when delays begin to exceed about 40 ms for the best lip-readers and about 80 ms for average lip-readers (see [46] and references there in). Therefore, previous methods in [27] and [28] (which employ appended delay in the forward path of DHAid) are not considered in the numerical experiments presented in this paper.

Fig. 7 shows impulse, magnitude, and phase response characteristics of the acoustic feedback paths used in numerical

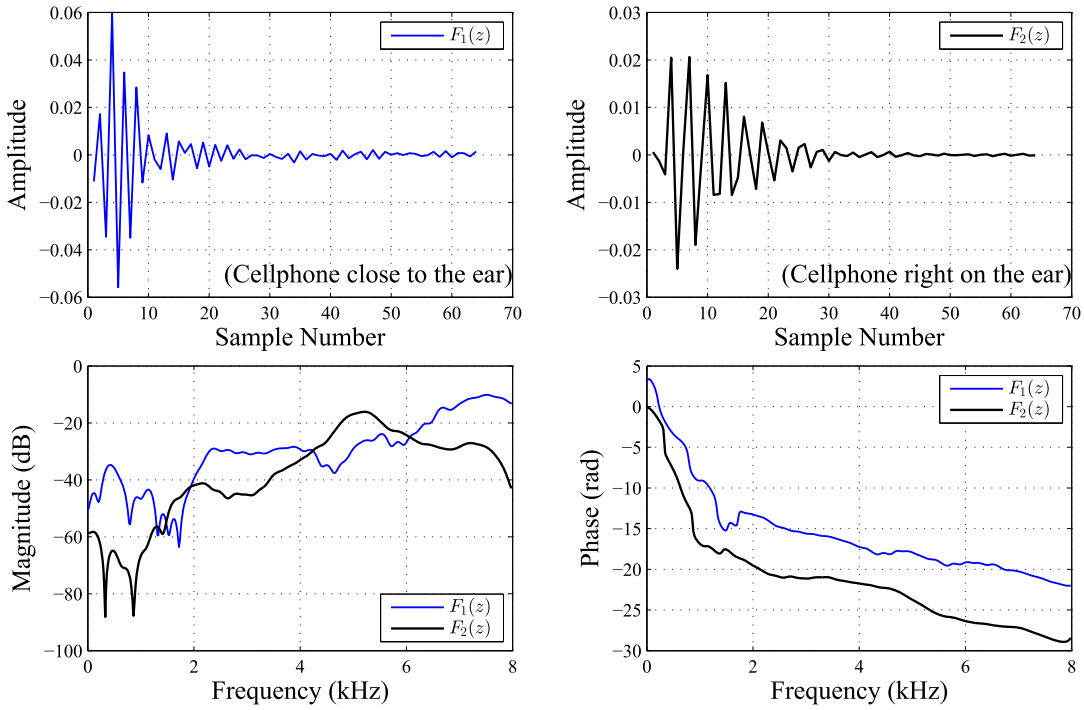

FIGURE 7. Characteristics of electro-acoustic feedback path $F(z)$ used in computer simulations. (top left) Impulse response characteristic of feedback path when the cellphone is close to ear, (top right) Impulse response characteristic of feedback path when the cellphone is right on the ear, (bottom left) the corresponding magnitude response characteristics, and (bottom right) the corresponding phase response characteristics.

experiments explained below. Here $F_1(z)$ denotes the acoustic feedback characteristics for the situation when user brings cellphone near to his/her ear, and $F_2(z)$ corresponds to the situation when the cellphone is right on the ear. The data for the acoustic paths is obtained from a freely available source[1] with full description available in [45]. The data obtained is preprocessed for the desired sampling frequency of $F_s = 16$ kHz, and truncation has been carried out to achieve the impulse response of length $L = 64$ as shown in Figs. 7(a) and 7(b). All adaptive filters are FIR filters of length $L = 64$ (same as that of the true acoustic feedback path(s)), except for the auxiliary AFC filter $V(z)$ in the basic (previous) and proposed methods. Due to the presence of the appended delay in the path for probe signal, the length of FIR auxiliary filter $V(z)$ is $L + D + 1 = 64 + 64 + 1 = 129$.

B. PERFORMANCE MEASURES

The convergence characteristics of various methods has been studied via *misalignment* between the true feedback path and its estimate provided by the adaptive filter being computed as NSD:

$$\text{NSD}(n) = 10\log\left\{\frac{\|\boldsymbol{f}(n) - \hat{\boldsymbol{f}}(n)\|^2}{\|\boldsymbol{f}(n)\|^2}\right\}, \tag{32}$$

[1] https://openspeechplatform.ucsd.edu/

where $\boldsymbol{f}(n)$ denotes coefficient vector of the true acoustic feedback path ($F_1(z)$ or $F_2(z)$ as used in a particular experiment), and $\hat{\boldsymbol{f}}(n)$ is the corresponding estimate provided by the adaptive AFC filter $H(z)$ in various methods as discussed in this paper. The most important objective of any DHAid device is to improve upon the gain available to user as the AFC system is put in action.

Another important performance metric is MSG being computed as

$$\text{MSG} = 10\log\left\{\max_{\omega}\|F(\omega) - \hat{F}(\omega)\|^2\right\}, \tag{33}$$

where $F(\omega)$ and $\hat{F}(\omega)$ denote the Fourier transform of the true acoustic feedback path $\boldsymbol{f}(n)$ and its estimate $\hat{\boldsymbol{f}}(n)$ obtained from the AFC filter, respectively. The frequency at which there is the most discrepancy between the true and estimated paths is used to calculate the MSG. The system won't be unstable, nevertheless, until the phase at that frequency is a multiple of 2π [24].

As shown in block diagrams (see Figs. 1-5), $x(n)$ is the desired input signal to be amplified for DHAid user, and $s(n)$ is the reconstructed signal being input to $G(z)$ and hence the DHAid received signal $u(n)$ is in fact an amplified version of $s(n)$. Therefore, the adaptive filtering AFC system must be efficient enough to mitigate the effect of acoustic feedback and ensure that $s(n)$ resembles $x(n)$ as close as possible. In order to perform the quantitative assessment of $s(n)$ in

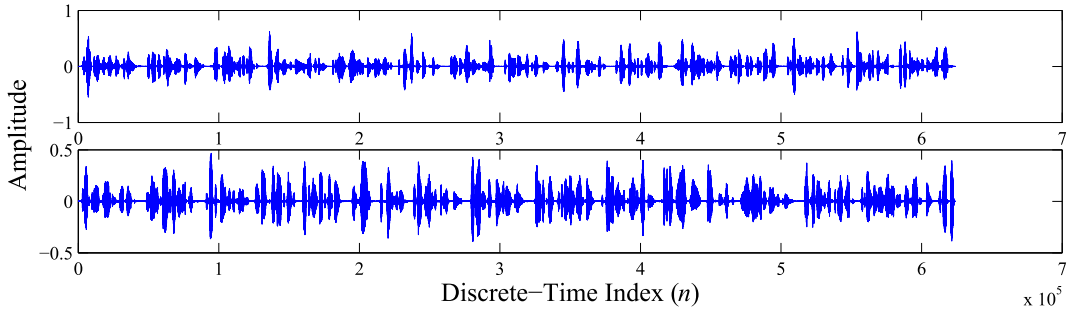

FIGURE 8. Speech signals from NOIZEUS database: (top) concatenated female speech signal, and (bottom) concatenated male speech signal.

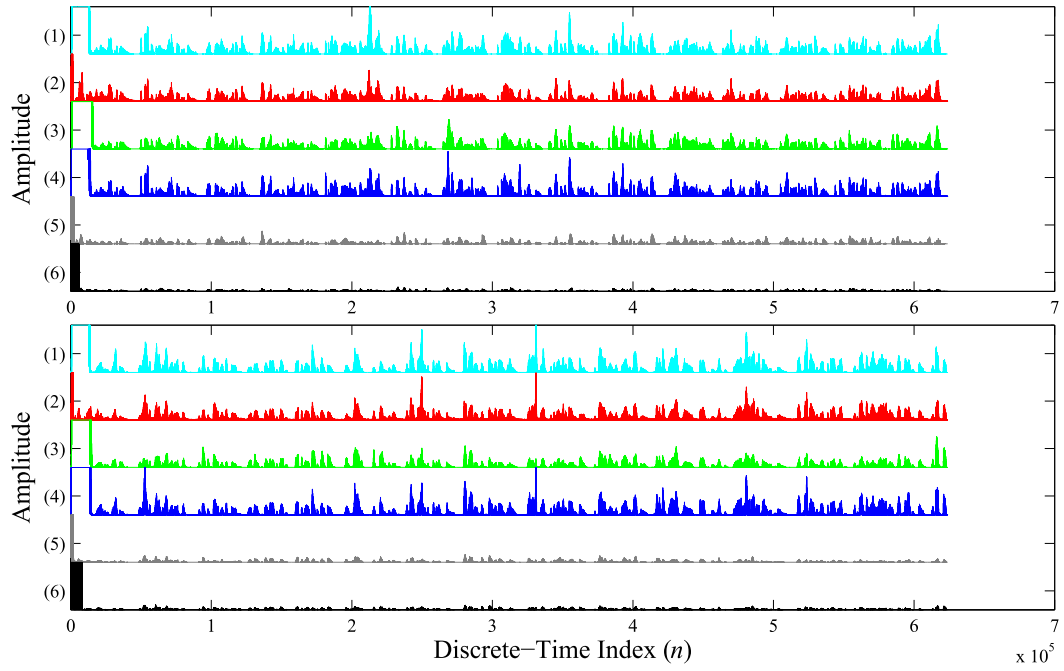

FIGURE 9. Simulations results for concatenated speech signals in Case 1 for DHAid with gain $K = 10$: The absolute difference (AD) between the source signal $x(n)$ and the reconstructed signal $s(n)$ being input to the HAid processing unit $G(z)$ for concatenated female speech signal (top) and for concatenated male speech signal (bottom). [(1) Conventional NLMS AFC, (2) Probe-shaping AFC, (3) PEM-AFC, (4) Basic method, (5) Proposed-a method, and (6) Proposed-b method.]

comparison with $x(n)$, various performance measures have been proposed in the literature on speech processing, where some of them have been developed specifically for signals in DHAid devices. We consider the following performance measures in this study:

- *Absolute Difference*: The visual inspection of the absolute difference (AD) being computed as

$$\text{AD}(n) = |x(n) - s(n)|, \tag{34}$$

  may give 'some' idea about the quality of the reconstructed signal $s(n)$.
- *Normalized Mean Squared Error*: The normalized mean squared error (NMSE) being computed (in dB) as

$$\text{NMSE} = 10 \log \left\{ \frac{\frac{1}{N} \sum_{n=n_0}^{n_0+N-1} [x(n) - s(n)]^2}{\frac{1}{N} \sum_{n=n_0}^{n_0+N-1} [x(n)]^2} \right\}, \tag{35}$$

where n_0 is selected when the AFC system have entered in its steady-state and N denotes the total number of samples selected for computation. Being a ratio of two similar quantities, NMSE is a unit-less quantity, and NMSE $\to -\infty$ shows that the corresponding signal is reconstructed with the minimum error.

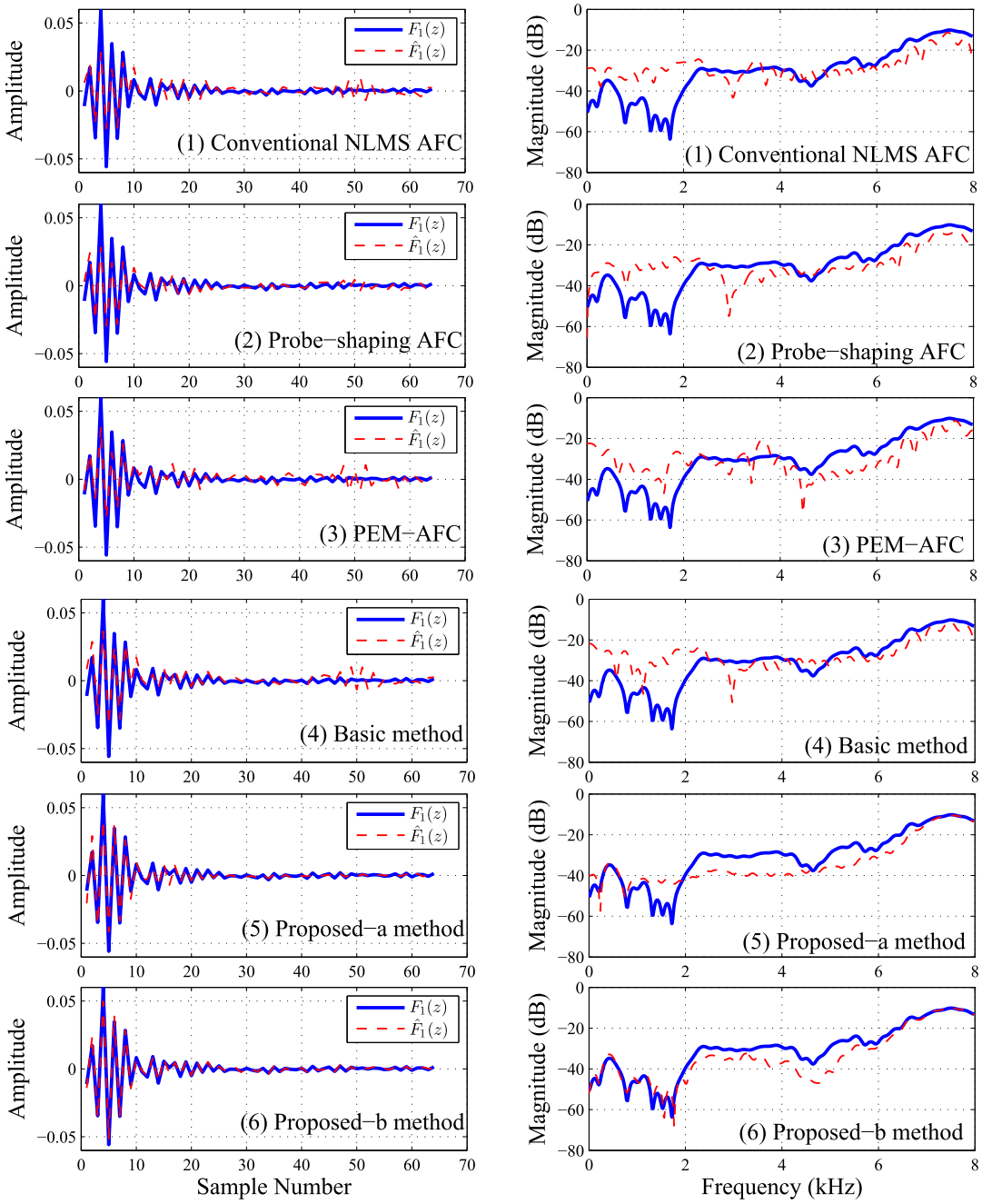

FIGURE 10. Simulations results for concatenated male speech signal in Case 1 for DHAid with gain $K = 10$: Impulse response (left column) and magnitude response (right column) characteristics of estimated acoustic feedback path $\hat{F}_1(z)$ (obtained by adaptive AFC filters in various methods) in comparison with the true acoustic feedback path $F_1(z)$.

- *Perceptual Evaluation of Speech Quality*: The AD as well as NMSE are not considered being robust performance metrics for non-stationary signals like speech, therefore, it is very important to consider other metrics which take statistical properties into consideration. The perceptual evaluation of speech quality (PESQ), an ITU-T standard for assessing the quality of speech signals, is one such criteria [47]. The highest score of 4.5 is given for a clean signal that has not been degraded.
- *Signal to Distortion Ratio*: The signal to distortion ratio (SDR) compares the levels of nonlinear distortion in the processed signal to the original signal, and is based on the Hilbert transform [48], [49], [50].
- *Mutual Information*: The Kullback-Leibler divergence can be used to interpret the mutual information (MI),

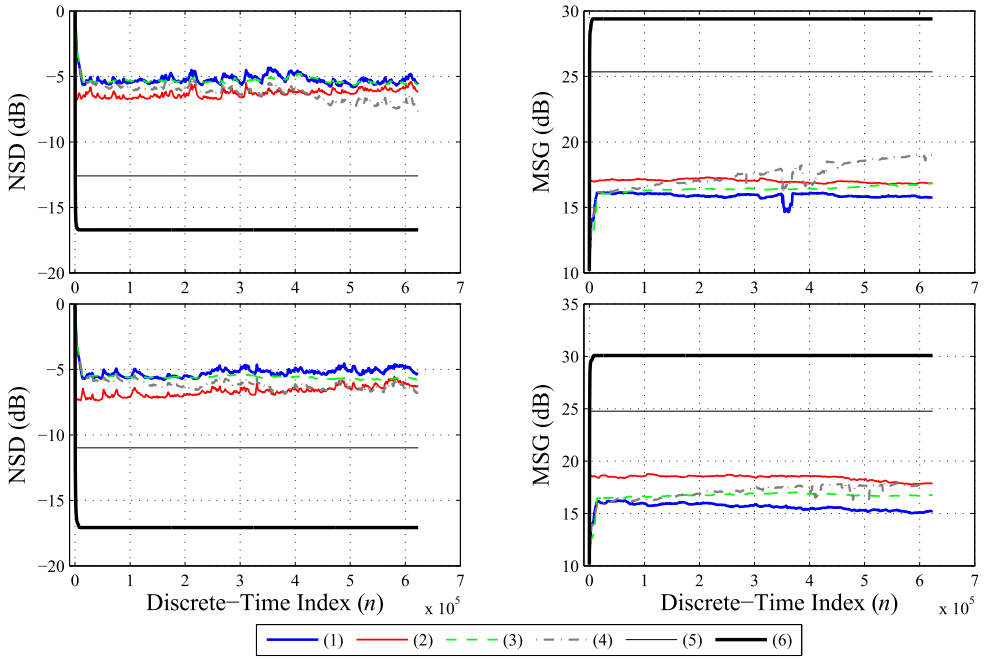

FIGURE 11. Simulations results for concatenated speech signals in Case 1 for DHAid with gain $K = 10$: (top-left) NSD (dB) curves for female speech signal, (top-right) MSG (dB) curves for female speech signal, (bottom-left) NSD (dB) curves for male speech signal, and (bottom-right) MSG (dB) curves for male speech signal. [(1) Conventional NLMS AFC, (2) Probe-shaping AFC, (3) PEM-AFC, (4) Basic method, (5) Proposed-a method, and (6) Proposed-b method.]

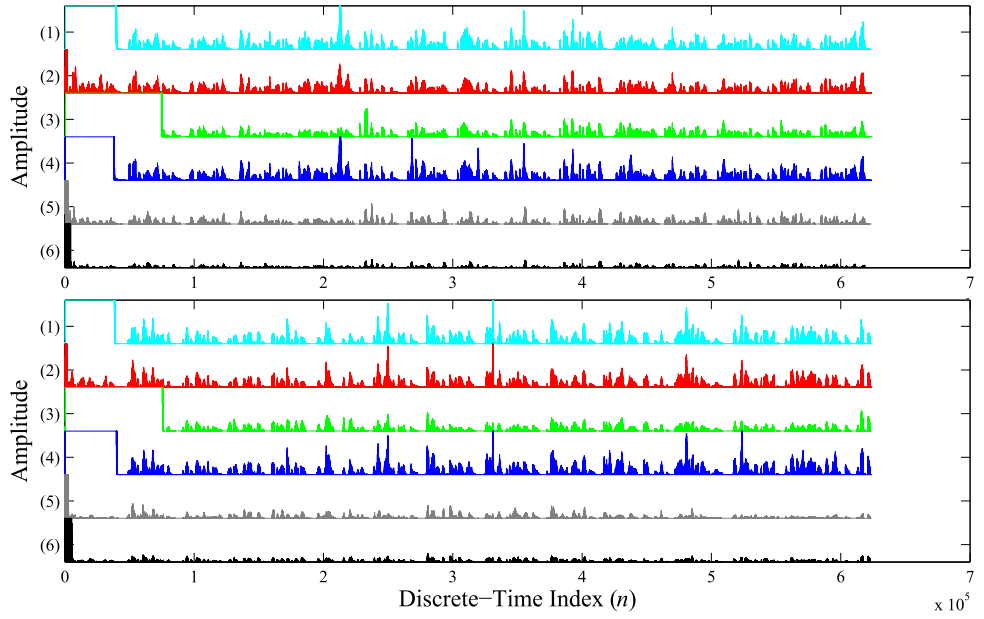

FIGURE 12. Simulations results for concatenated speech signals in Case 1 for DHAid with gain $K = 20$: The absolute difference (AD) between the source signal $x(n)$ and the reconstructed signal $s(n)$ being input to the HAid processing unit $G(z)$ for concatenated female speech signal (top) and for concatenated male speech signal (bottom). [(1) Conventional NLMS AFC, (2) Probe-shaping AFC, (3) PEM-AFC, (4) Basic method, (5) Proposed-a method, and (6) Proposed-b method.]

a non-parametric measure of similarity between two random variables X and Y, as [51]

$$\mathrm{MI} = \int_{-\infty}^{\infty}\int_{-\infty}^{\infty} f(X,Y)\log\left(\frac{f(X,Y)}{f(X)f(Y)}\right)dXdY, \quad (36)$$

where the joint probability distribution function of X and Y is denoted by $f(X,Y)$, and the marginal probability distribution functions (PDFs) of X and Y are denoted by $f(X)$ and $f(Y)$, respectively. MI is always non-negative and zero if and only if the two random

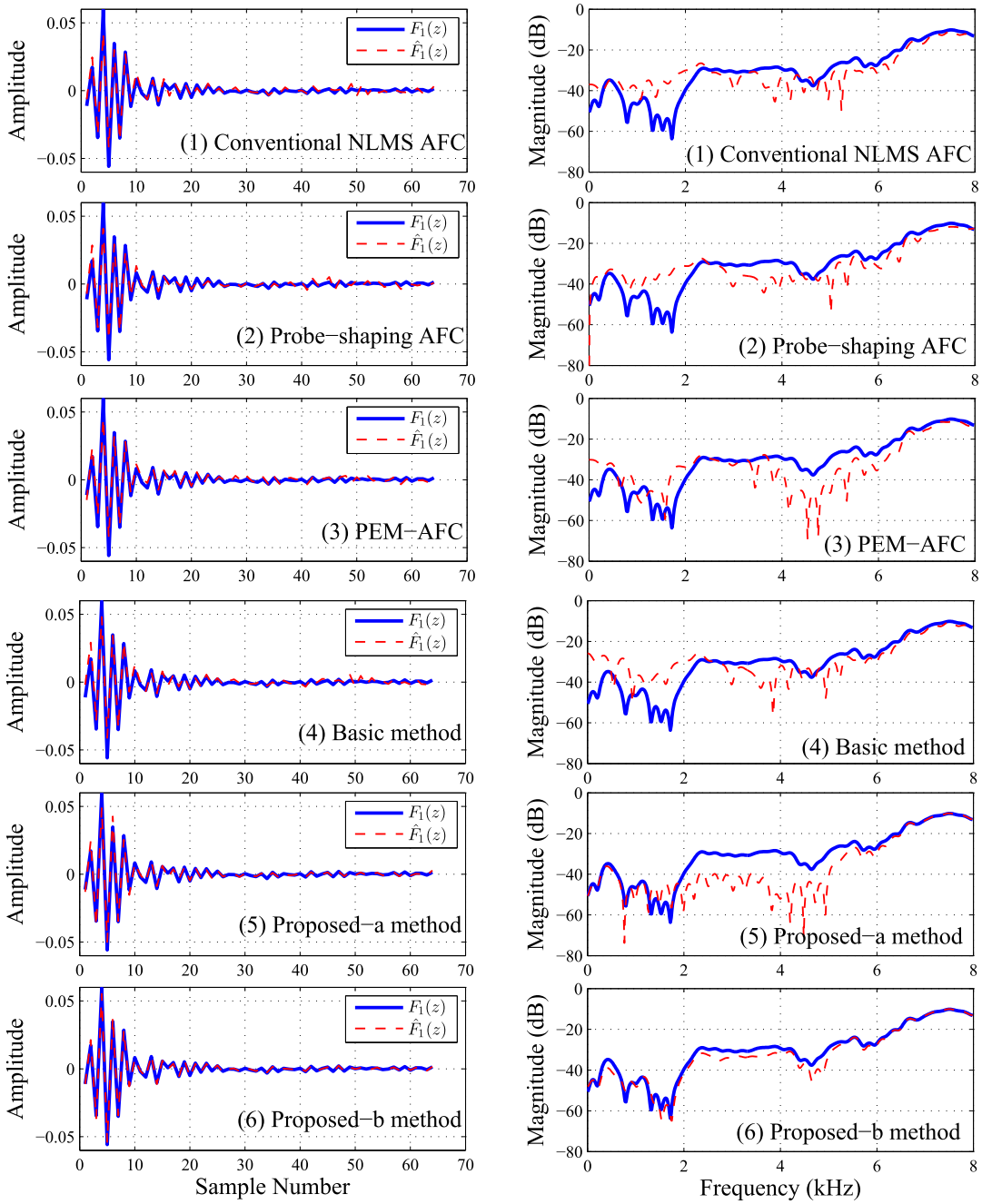

FIGURE 13. Simulations results for concatenated male speech signal in Case 1 for DHAid with gain $K = 20$: Impulse response (left column) and magnitude response (right column) characteristics of estimated acoustic feedback path $\hat{F}_1(z)$ (obtained by adaptive AFC filters in various methods) in comparison with the true acoustic feedback path $F_1(z)$.

variables are strictly independent. With the knowledge that (MI > 0) signifies a close match between 'signals', we compute MI between the input signal $x(n)$ and the reconstructed signal $s(n)$. The larger the MI, the more closely the reconstructed signal $s(n)$ resembles the input signal $x(n)$.

- *Hearing Aid Speech Quality Index*: An index created specifically for the speech signals processed by DHAid devices is the hearing aid speech quality index (HASQI). HASQI has been created to foresee changes in speech quality due to noise, nonlinear distortions, frequency compression-related degradations, speech vocoding, noise suppression, acoustic feedback and feedback cancellation, and speech mixed with modulated noise. For a clear signal with no deterioration, the maximum score is 1.0 [52], [53].

TABLE 3. Quantitative assessment of various methods for concatenated female speech signals from NOIZEUS database in Case 1.

	$(K = 10)$						$(K = 20)$					
Method	HASQI	HAAQI	PESQ	SDR	MI	NMSE	HASQI	HAAQI	PESQ	SDR	MI	NMSE
(1)	0.8139	0.7820	3.2945	9.0395	0.8002	-7.7761	0.8152	0.7802	3.3097	8.9292	0.7558	-7.7565
(2)	0.8563	0.7663	3.0875	10.7960	0.8846	-9.8279	0.8551	0.7987	3.3159	10.7508	0.8937	-9.6655
(3)	0.8444	0.8327	3.7239	12.8872	0.8437	-9.6095	0.8578	0.8814	4.0917	15.1504	0.9994	-10.6431
(4)	0.8084	0.7728	3.2605	10.0883	0.7934	-7.8536	0.7834	0.7655	3.2298	9.3338	0.7783	-7.0001
(5)	0.9616	0.9501	4.4648	**87.5541**	1.4149	-20.7463	0.9148	0.8221	4.2688	**83.6808**	1.2675	-16.0165
(6)	**0.9827**	**0.9861**	**4.4848**	75.7770	**1.6262**	**-28.0439**	**0.9765**	**0.9526**	**4.4591**	67.3006	**1.6825**	**-23.8723**

(1) Conventional NLMS AFC, (2) Probe-shaping AFC, (3) PEM-AFC,
(4) Basic method, (5) Proposed-a method, and (6) Proposed-b method.

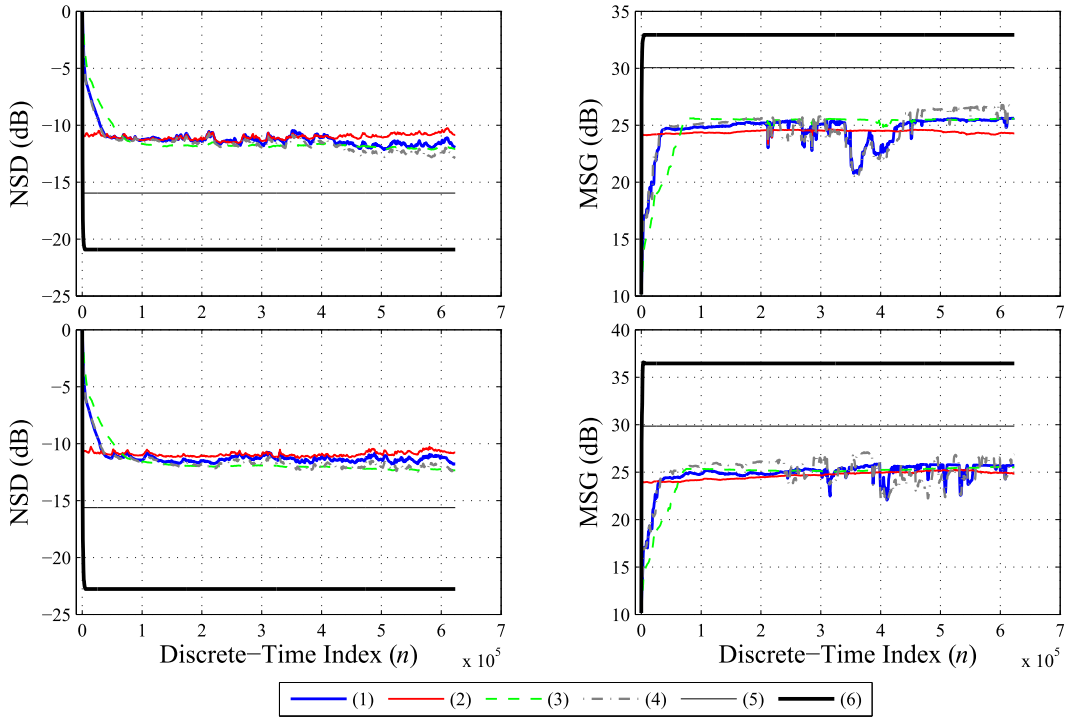

FIGURE 14. Simulations results for concatenated speech signals in Case 1 for DHAid with gain $K = 20$: (top-left) NSD (dB) curves for female speech signal, (top-right) MSG (dB) curves for female speech signal, (bottom-left) NSD (dB) curves for male speech signal, and (bottom-right) MSG (dB) curves for male speech signal. [(1) Conventional NLMS AFC, (2) Probe-shaping AFC, (3) PEM-AFC, (4) Basic method, (5) Proposed-a method, and (6) Proposed-b method.]

- *Hearing Aid Audio Quality Index*: The hearing aid audio quality index (HAAQI) has been created as a way to forecast the audio quality (particularly for music signals) in DHAid devices. It uses the HASQI auditory model with various parameters fitted to the results of a significant music-quality rating experiment [54]. If there is no signal deterioration, the maximum score is 1.0 [54].
- *Output SNR*: For probe-signal based AFC methods (probe-shaping NLMS [21], basic method [44], and proposed method), it is very important to compute the output SNR as

$$\text{SNR\_out} = 10\log\left\{\frac{\sigma_u^2}{\sigma_p^2}\right\}, \tag{37}$$

where σ_u^2 and σ_p^2 denote variances of the received signal $u(n)$ and the probe signal $p(n)$, respectively.

C. CASE 1: LONG SPEECH SIGNALS

The objective of this case study is to understand the performance of various AFC methods for long speech signals. The clean speech signals provided in the NOIZEUS[2] database (available free of charge) [55] are used for this purpose. Essentially, fifteen clean speech signals spoken by female speakers are concatenated to obtain a long female speech signal, and fifteen clean speech signals spoken by male speakers are concatenated to obtain a long male speech signal. The waveplots for these signals are shown in Fig. 8, and the simulation results have been carried out using acoustic feedback path $F_1(z)$ (see Fig. 7.).

Fig. 9 shows curves for AD (as defined in (34)) for various AFC methods for DHAid with gain $K = 10$. For sake of

[2]https://ecs.utdallas.edu/loizou/speech/noizeus/

TABLE 4. Quantitative assessment of various methods for concatenated male speech signals from NOIZEUS database in Case 1.

	$(K = 10)$						$(K = 20)$					
Method	HASQI	HAAQI	PESQ	SDR	MI	NMSE	HASQI	HAAQI	PESQ	SDR	MI	NMSE
(1)	0.7995	0.8170	3.8928	9.7586	0.8728	-6.9783	0.7992	0.8127	3.9081	9.7454	0.8800	-7.0167
(2)	0.8331	0.7862	3.4787	10.8779	0.9187	-8.4504	0.8193	0.8123	3.7144	10.5913	0.8705	-7.8750
(3)	0.8689	0.8973	4.2573	15.6318	1.0510	-10.5573	0.8876	0.9217	4.3559	18.2964	1.1630	-12.2689
(4)	0.7824	0.8093	3.9205	10.7373	0.8643	-6.9671	0.7668	0.7914	3.8429	9.8078	0.8234	-6.2470
(5)	**0.9780**	0.9580	**4.4902**	77.0534	**1.9463**	-25.1353	0.9387	0.8271	4.3701	**70.2996**	1.6092	-19.3556
(6)	0.9733	**0.9771**	4.4760	**77.5602**	1.7809	**-25.6082**	**0.9625**	**0.9519**	**4.4485**	69.7014	**1.6765**	**-19.7482**

(1) Conventional NLMS AFC, (2) Probe-shaping AFC, (3) PEM-AFC,
(4) Basic method, (5) Proposed-a method, and (6) Proposed-b method.

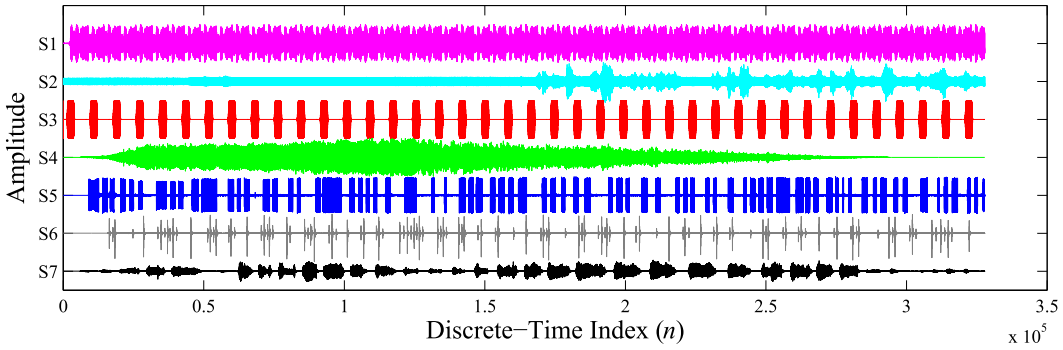

FIGURE 15. Plots for mixed characteristic audio signals used in the computer simulations in Case 2.

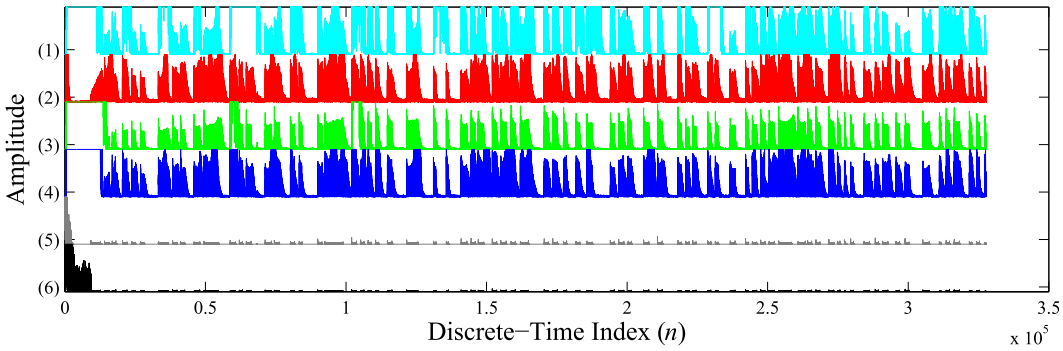

FIGURE 16. Simulations results for signal S5 in Case 2 for DHAid with gain $K = 10$: The absolute difference (AD) between the source signal $x(n)$ and the reconstructed signal $s(n)$ being input to the HAid processing unit $G(z)$ for (1) Conventional NLMS AFC, (2) Probe-shaping AFC, (3) PEM-AFC, (4) Basic method, (5) Proposed-a method, and (6) Proposed-b method.

TABLE 5. Comparison of SNR_out for various probe signal-based methods for concatenated speech signals from NOIZEUS database in Case 1.

	female speech		male speech	
	$(K = 10)$	$(K = 20)$	$(K = 10)$	$(K = 20)$
Probe-shaping AFC	14.7534	20.6086	15.4812	21.6086
Basic method	34.1218	40.2769	35.0676	41.1776
Proposed-a method	**96.0784**	**96.7852**	**87.8425**	**95.1329**
Proposed-b method	79.2316	77.1374	83.8183	80.2671

space, all signals are plotted in the same panel (by shifting the signals) on the scale of 0 to 1 for each signal. Though visual inspections cannot reveal true quality and efficacy of the AFC algorithm in removing the acoustic feedback, it is evident that the proposed methods perform better in comparison with the rest of methods considered in this paper. The characteristics of estimated acoustic feedback path $\hat{F}_1(z)$ obtained by AFC adaptive filter (in various methods) at steady-state in comparison with the true acoustic feedback path $F_1(z)$ are shown in Fig. 10 for male speech signals (the curves for female signals have been omitted), where both the impulse response and the corresponding magnitude response characteristics have been plotted. It is noticed that all methods considered in this paper are able to converge to a reasonable estimate of the acoustic feedback path for only a certain range of frequencies. On the other hand, the proposed method demonstrates better estimate

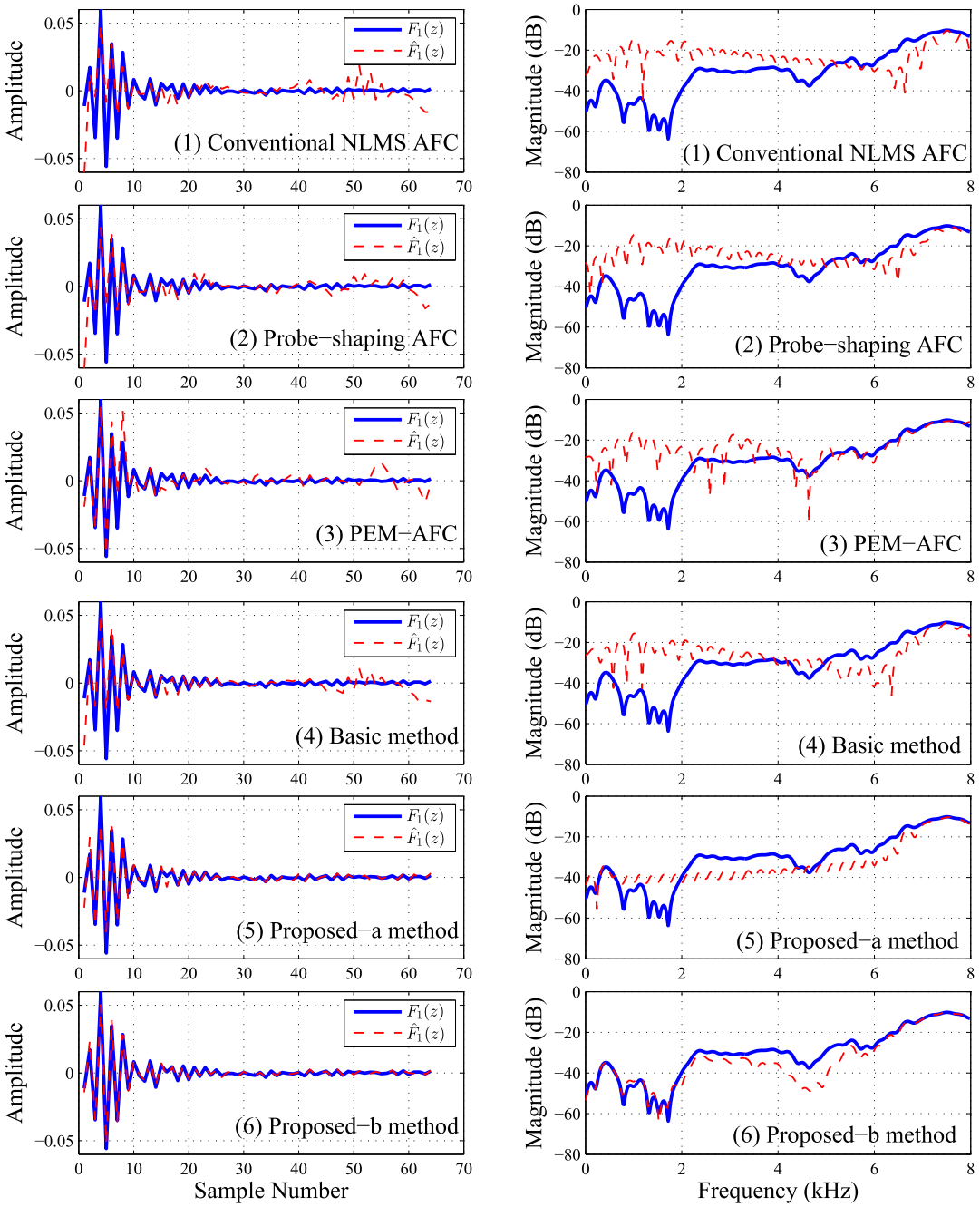

FIGURE 17. Simulations results for signal S5 in Case 2 for DHAid gain $K = 10$: Impulse response (left column) and magnitude response (right column) characteristics of estimated acoustic feedback path $\hat{F}_1(z)$ (obtained by adaptive AFC filters in various methods) in comparison with the true acoustic feedback path $F_1(z)$.

as compared with the rest of methods for the whole frequency range.

The convergence curves for NSD and MSG, as defined in (32) and (33), respectively, are shown in Fig. 11. It is observed that the proposed method exhibits fast convergence speed as well as best steady-state performance as compared with the rest of methods. The comparison between two versions of proposed methods, i.e. proposed-a and proposed-b, reveals that incorporating the MVC-based adaptive filtering for adaptation of send AFC filter $V(z)$ indeed offers some performance benefits in terms of better steady-state performance in comparison with if MVC-based adaptive filtering were not employed. It is worth to mention that 'good' NSD performance means 'good' estimation of acoustic feedback path (as observed in Fig. 10 by directly plotting the adaptive filters' coefficients and magnitude response characteristics).

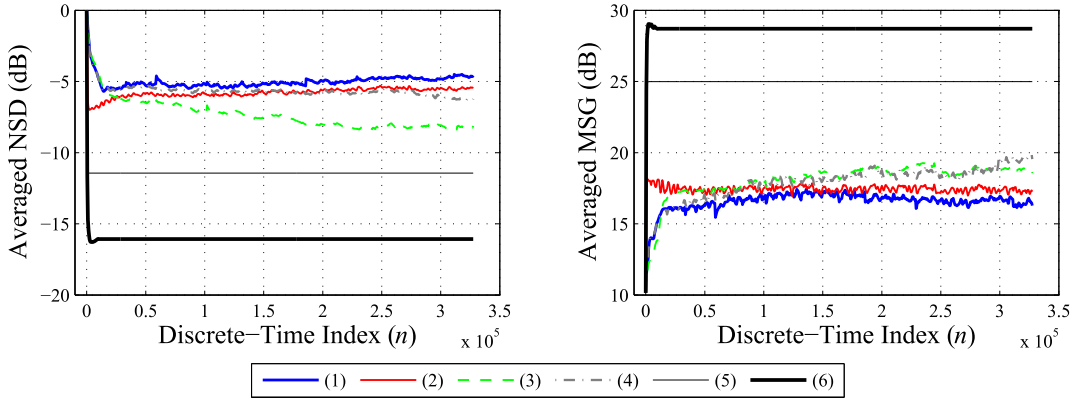

FIGURE 18. Averaged NSD and MSG curves in Case 2 for DHAid with gain $K = 10$. [(1) Conventional NLMS AFC, (2) Probe-shaping AFC, (3) PEM-AFC, (4) Basic method, (5) Proposed-a method, and (6) Proposed-b method.]

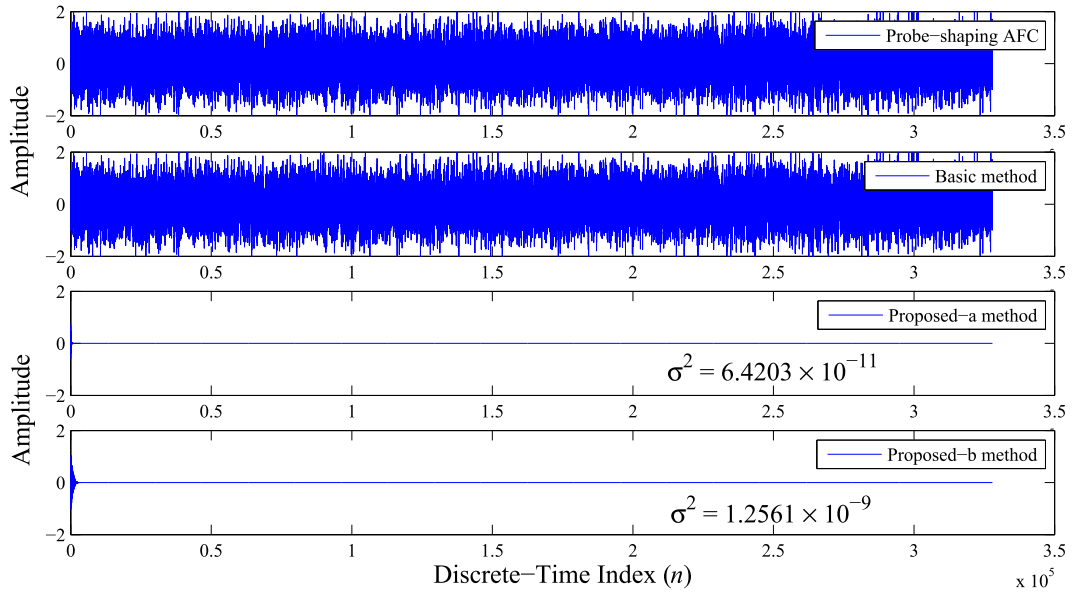

FIGURE 19. Variation of probe signal $p(n)$ in probe signal-based methods for signal S5 in Case 2 for DHAid with gain $K = 10$.

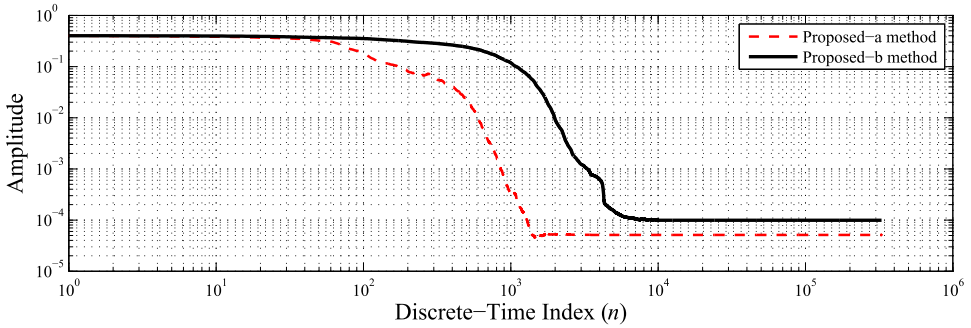

FIGURE 20. Variation of the gain control parameter $\beta(n)$ in proposed method averaged over all signals in Case 2 for DHAid with gain $K = 10$.

Furthermore, 'good' MSG performance would indicate that the DHAid would allow 'high' level of gain in the DHAid processing unit if the AFC system is in action.

The above-detailed experiment for concatenated speech signals for acoustic feedback path $F_1(z)$ has been repeated for a DHAid with gain $K = 20$. The corresponding simulation

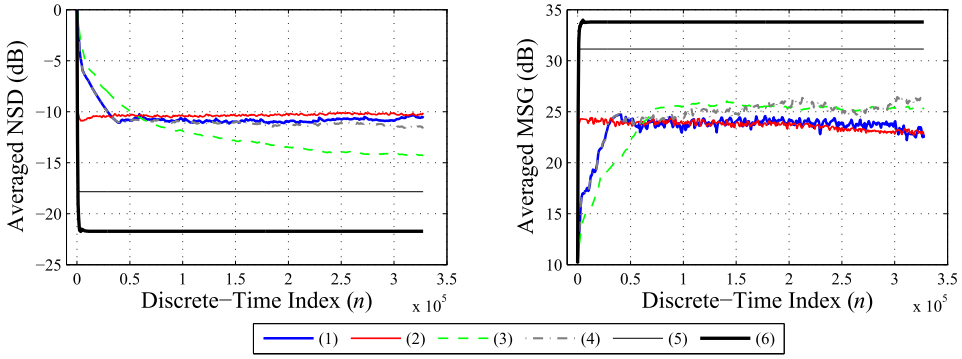

FIGURE 21. Averaged NSD and MSG curves in Case 2 for DHAid with gain $K = 20$. [(1) Conventional NLMS AFC, (2) Probe-shaping AFC, (3) PEM-AFC, (4) Basic method, (5) Proposed-a method, and (6) Proposed-b method.]

TABLE 6. Comparison of SNR_out for various probe signal-based methods for experiments carried out in Case 2.

		Probe-shaping AFC	Basic method	Proposed-a method	Proposed-b method
$K = 10$	S1	14.9608	34.8776	**111.8545**	80.6990
	S2	14.3641	35.6784	86.1135	**91.6134**
	S3	15.7861	35.0562	89.9889	**98.6232**
	S4	15.7288	35.0732	**93.7786**	92.6521
	S5	12.2146	33.1932	**113.5709**	100.6855
	S6	16.7408	35.5519	**87.6473**	78.0907
	S7	15.8699	35.1447	**83.8515**	81.4890
	Mean	15.0950	34.9393	**95.2579**	89.1218
	SD	01.3647	00.7605	11.4168	08.3969
	Median	15.7288	35.0732	89.9889	**91.61341**
$K = 20$	S1	20.3858	40.9049	**117.1561**	85.5473
	S2	19.9222	40.4601	**94.6172**	85.1276
	S3	21.6632	41.2010	**106.0680**	102.9207
	S4	21.3555	41.1241	**116.9565**	104.7476
	S5	16.6924	47.1121	**119.0452**	109.3287
	S6	22.8017	41.9076	**96.6618**	87.9829
	S7	21.9475	41.3811	**107.0947**	94.4723
	Mean	20.6812	42.0130	**108.2285**	95.7325
	SD	01.8552	02.1213	09.2419	09.2245
	Median	21.3555	41.2010	**107.0947**	94.4723

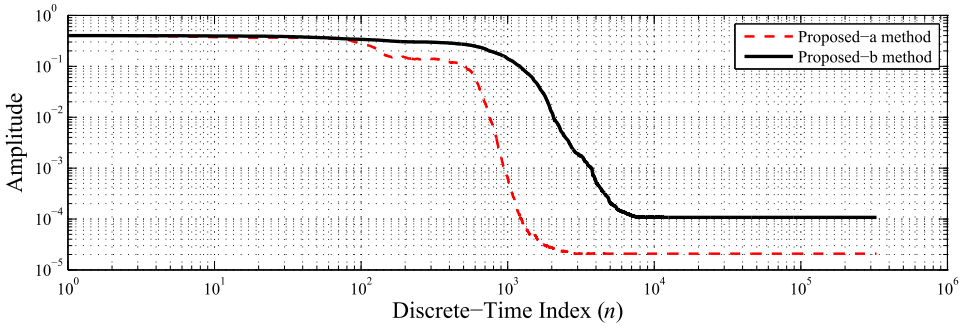

FIGURE 22. Variation of the gain control parameter $\beta(n)$ in proposed method averaged over all signals in Case 2 for DHAid with gain $K = 20$.

results are presented in Figs. 12-14. Fig. 12 plots comparison for AD between the input signal $x(n)$ and DHAid input signal $s(n)$ for various methods. It is observed that conventional NLMS AFC, PEM-AFC, and basic method take a long time to recover from the initial howling period under this high gain scenario. It is important to mention that plotted signals

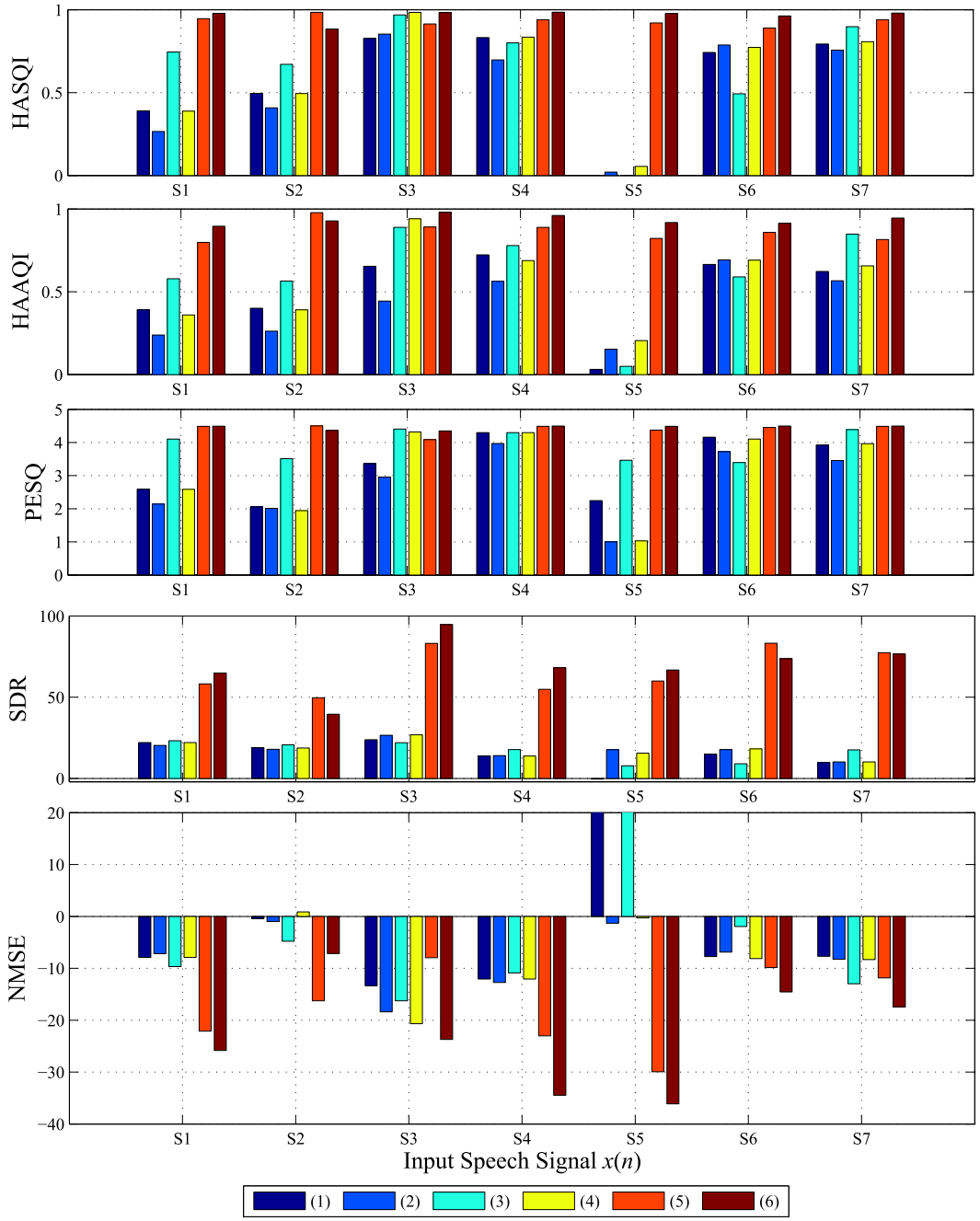

FIGURE 23. Bar plots for various AFC methods for all signals (S1-S7) in Case 2 for DHAid gain $K = 10$. [(1) Conventional NLMS AFC, (2) Probe-shaping AFC, (3) PEM-AFC, (4) Basic method, (5) Proposed-a method, and (6) Proposed-b method.]

have been clipped (with a same threshold for all methods for a fair comparison) for better visual presentation; otherwise, very high oscillations have been observed during the howling period. The prob-shaping AFC, proposed-a and proposed-b are able to recover quickly from the initial howling period. Furthermore, the proposed methods exhibits smallest reconstruction error between $x(n)$ and $s(n)$ among the methods considered in this paper. Fig. 13 shows steady-state impulse and magnitude response characteristics of estimate $\hat{F}_1(z)$ in comparison with $F_1(z)$. As observed previously for $K = 10$, the adaptive AFC filter in the proposed method converges to a solution which matches closely with the true acoustic feedback path for almost all frequencies in consideration. Finally, Fig. 14 shows the convergence curves for NSD and MSG, which show that the proposed method shows better performance, in comparison with that of the other methods, for fast convergence speed and good steady-state performance.

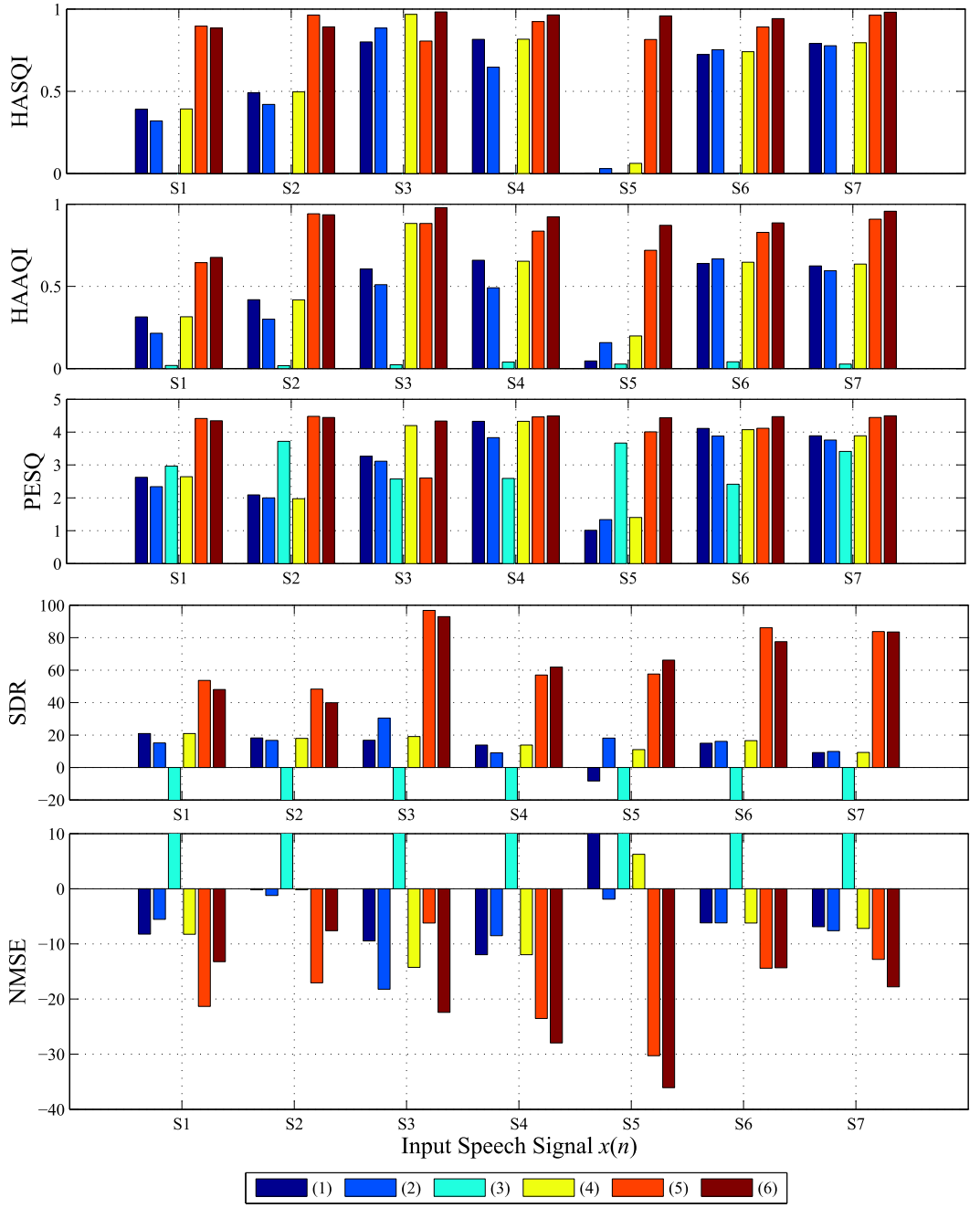

FIGURE 24. Bar plots for various AFC methods for all signals (S1-S7) in Case 2 for DHAid gain $K = 20$. [(1) Conventional NLMS AFC, (2) Probe-shaping AFC, (3) PEM-AFC, (4) Basic method, (5) Proposed-a method, and (6) Proposed-b method.]

The quantitative assessment of various methods, from the view point of reconstruction quality of the DHAid input signal $s(n)$ in comparison with the input signal $x(n)$ being treated as a ground truth, is summarized in Tables 3 and 4. Here 'boldface' ('underline') is used to signify the best (2nd-best) results achieved. It is observed that the existing AFC methods (conventional NLMS, probe-shaping NLMS, PEM-AFC, and basic method) show a mixed performance from the view point of showing better performance for some measures than for the others. The proposed methods show considerably improved performance for all performance measures, with proposed-b (full) method showing better (or comparable) performance than that of the proposed-a method. The performance comparison from the view point of SNR_out (comparing power of DHAid received signal $u(n)$ with respect to the probe signal) for probe signal-based methods is presented in Table 5. It is noticed that the proposed methods give far more better performance than the probe-shaping NLMS and the basic method.

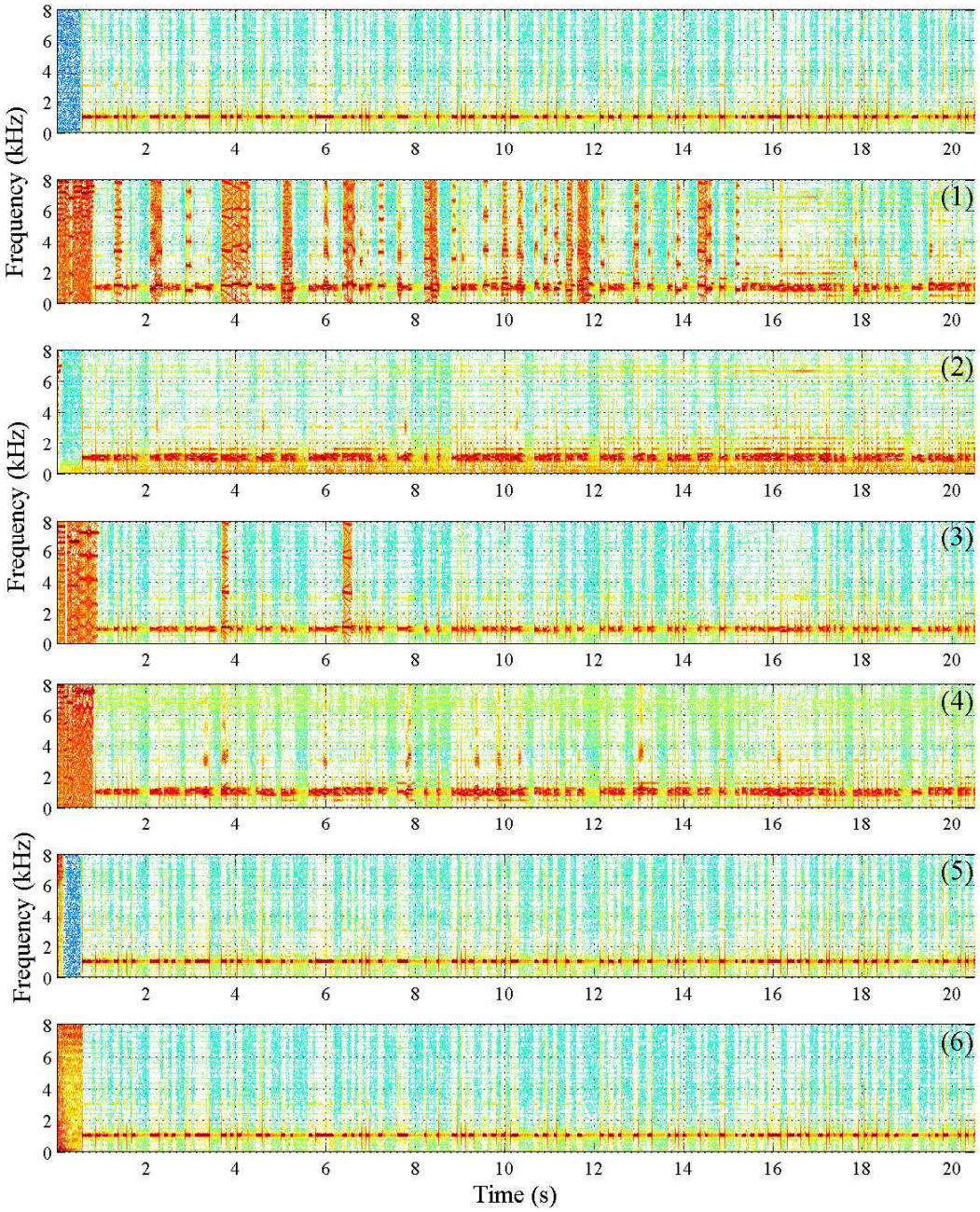

FIGURE 25. Spectrogram of input signal S5 (top) in comparison with spectrogram of DHAid input signal $s(n)$ in (1) Conventional NLMS AFC, (2) Probe-shaping AFC, (3) PEM-AFC, (4) Basic method, (5) Proposed-a method, and (6) Proposed-b method, for simulations in Case 2 for DHAid with gain $K = 10$.

Thanks to the gain control strategy for the probe signal, the level of probe signal reduces to a very low level as the AFC system reaches steady-state. Our experience shows that the random noise present 60 dB below than the desired signal is not perceivable by human ear. The proposed method reduces the probe signal to a very low level not at all audible, and therefore holds promise for practical DHAid devices.

D. CASE 2: MIXED-CHARACTERISTICS AUDIO SIGNALS

In this case study, we consider mixed characteristic audio signals as shown in Fig. 15. The description of various signals presented therein is as follows: S1 is an ambulance siren, S2 is strong tonal signal with some speech signal present in the later half of signal, S3 is of impulsive signal with periodic tones, S4 is a mix of police siren with an ambulance siren present in the background, S5 is an impulsive signal with quasi-periodic tones, S6 is a sound recorded from a typewriter, and S7 is a very shrilling sound from a barking puppy. It is worth to mention that such signals pose a great challenge for DHAid devices for the very annoying entrainment artifacts [12]. The entrainment artifacts include whistle-like sounds that may or may not be harmonically related to

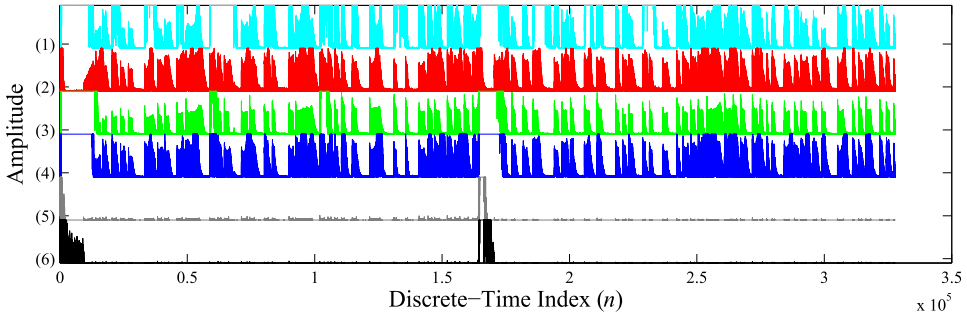

FIGURE 26. Simulations results for signal S5 in Case 3 for a sudden change in the acoustic path with gain $K = 10$: The absolute difference (AD) between the source signal $x(n)$ and the reconstructed signal $s(n)$ being input to the HAid processing unit $G(z)$ for (1) Conventional NLMS AFC, (2) Probe-shaping AFC, (3) PEM-AFC, (4) Basic method, (5) Proposed-a method, and (6) Proposed-b method.

the input tonal signal. These artifacts are very annoying to the DHAid users, and can result in a reduced output signal quality [56]. As in the previous case study, the experiments have been performed for the acoustic feedback path $F_1(z)$ (as shown in Fig. 7) for DHAid gain $K = 10$ and $K = 20$.

Fig. 16 shows performance comparison from the view point of AD (34) for signal S5, which shows superior performance of the proposed method resulting in reduced reconstruction error in the input signal for the DHAid. Fig. 17 plots the impulse and magnitude response characteristics of estimate $\hat{F}_1(z)$ at the steady-state in comparison with the true acoustic feedback path $F_1(z)$. It is evident that the proposed method keeps the good performance in identifying the characteristic of the feedback path even for such a challenging input signal. The corresponding convergence curves for NSD and MSG averaged for all signals shown in Fig. 15 are shown in Fig. 18. It is observed that the proposed method clearly outperforms the rest of methods both in convergence speed as well as the steady-state performance. Among the proposed method variants a and b, the proposed-b method gives better performance than that of the proposed-a method, thanks to MVC-based hybrid adaptive filtering for adaptation of the auxiliary AFC filter. Fig. 19 shows variation of probe signal is all probe signal-based methods, and Fig. 20 shows variation of gain control parameter $\beta(n)$ in the proposed method. It is observed that the proposed method reduces the strength of the probe signal as the AFC converges (see variance of probe signal given in the corresponding subfigure), thanks to the gain control parameter in the proposed method. This in turn improves the SNR_out performance in the proposed method.

The above detailed experiment is repeated for DHAid with a high gain value of $K = 20$. The results for individual signals are omitted and only averaged results are discussed below. Fig. 21 shows convergence curves for NSD and MSG averaged for all signals S1-S7 (shown in Fig. 15), and the corresponding curves for the variation of gain control parameter $\beta(n)$ in the proposed method(s) are shown in Fig. 22. A similar performance comparison is observed as in the pervious experiments, i.e., the proposed method gives the best performance among the methods considered in this paper. It achieves fast convergence speed and best steady-state values for both NSD and MSG. Furthermore, the gain control parameter converges to a very small value as the AFC system converges, this reduces the strength of the probe signal at the steady-state and hence improves the SNR_out. This is indeed observed from the results presented in Table 6, that the proposed method substantially improves upon the SNR_out as compared with the existing methods involving probe signal.

Considering the mixed nature of signals considered in this case study, we employ bar plots to show performance of various methods for individual signals for various other performance measures. Fig. 23 shows bar plots for HASQI, HAAQI, PESQ, SDR and NMSE for all signals S1-S7 (shown in Fig. 16) considered in this case study for DHAid with gain $K = 10$. The varying degree of performance on the basis of various performance measures signifies that 'averaged' results on the basis of NSD and/or MSG may be misleading. The first observation is that the proposed method exhibits better performance than the rest of methods for almost all signals and on the basis of all performance measures. Another interesting observation is performance comparison for signals S2 (tonal signal with speech content) and S5 (impulsive quasi-periodic tonal signal). The corresponding results for a high gain scenario of $K = 20$ are presented in Fig. 24. The PEM-AFC shows very poor performance from the view point of SDR and NMSE. As in the previous case for $K = 10$, the proposed method keeps the good and stable performance.

As stated earlier, the DHAid device may suffer from entrainment artifacts when excited with an input signal having tonal characteristics or musical content. As a typical example, lets revisit the performance of various methods for signal S5 for $K = 10$. In order to understand the frequency domain behavior of various methods, the spectrograms for reconstructed signal $s(n)$ (which is input to the DHAid processing unit) for various methods, in comparison with the spectrogram of the (reference) input signal $x(n)$, are plotted in Fig. 25. It is observed that the performance of the existing methods is very poor, and in fact, the existing methods suffer from a lot of entrainment artifacts. The proposed method is

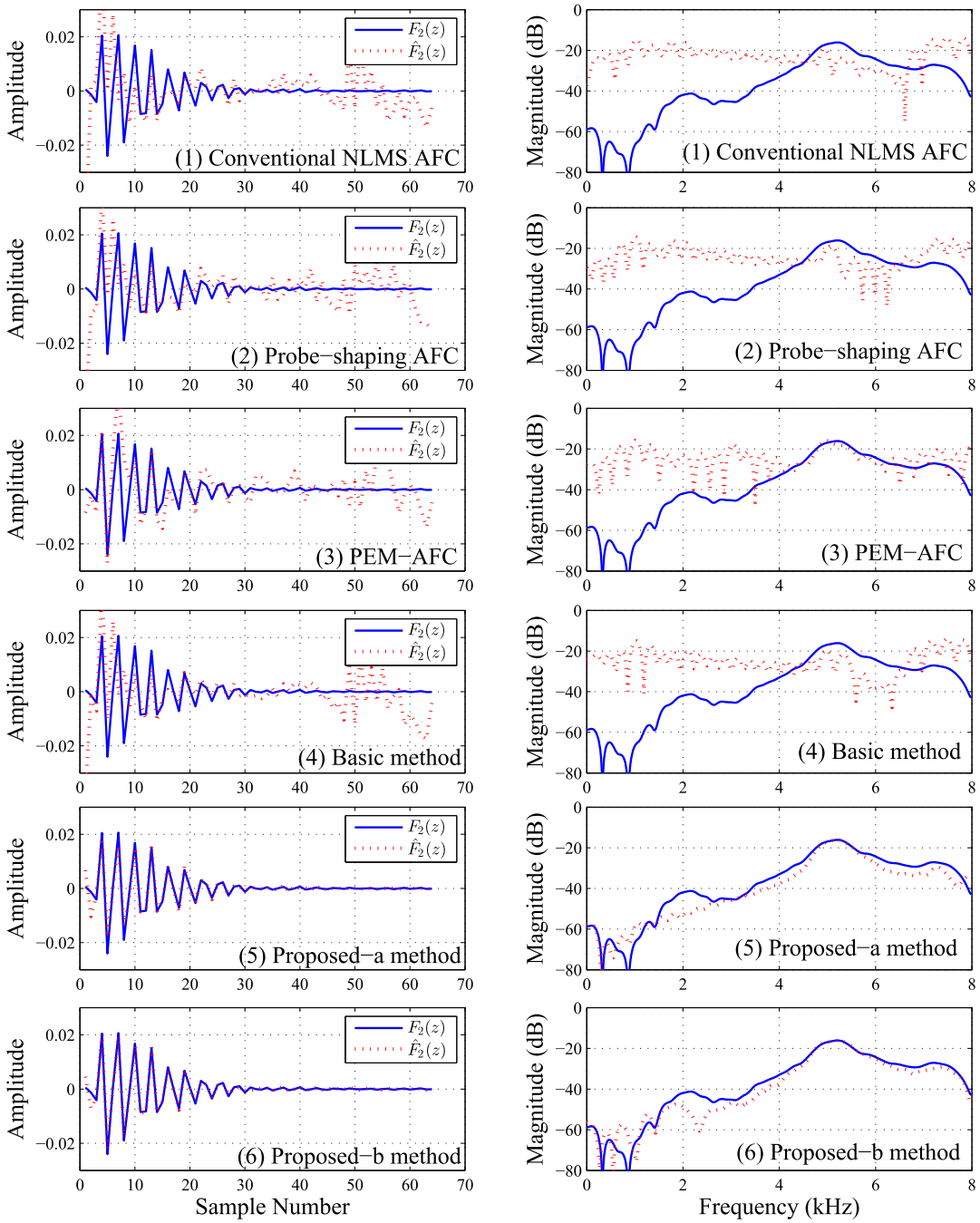

FIGURE 27. Simulations results for signal S5 in Case 3 for a sudden change in the acoustic path with gain $K = 10$: Impulse response (left column) and magnitude response (right column) characteristics of estimated acoustic feedback path $\hat{F}_2(z)$ (obtained by adaptive AFC filters in various methods) in comparison with the true acoustic feedback path $F_2(z)$.

every efficient is this regard, in fact, no extra tone is heard when listening to the reconstructed signal from the proposed AFC method.

E. CASE 3: SUDDEN CHANGE IN ACOUSTIC PATH CHARACTERISTICS

So far, we have assumed that the acoustic feedback path is an LTI system, and the objective of experiments have been to understand convergence and steady-state performance of various adaptive AFC methods. However, it is very important to study the tracking performance of any adaptive system for time-varying systems, and this is indeed the main objective of this case study. As shown in Fig. 7, $F_1(z)$ is the transfer function of the acoustic feedback path measured under the situation when DHAid user brings a cellphone close to ear, and $F_2(z)$ corresponds to situation when the cellphone is right

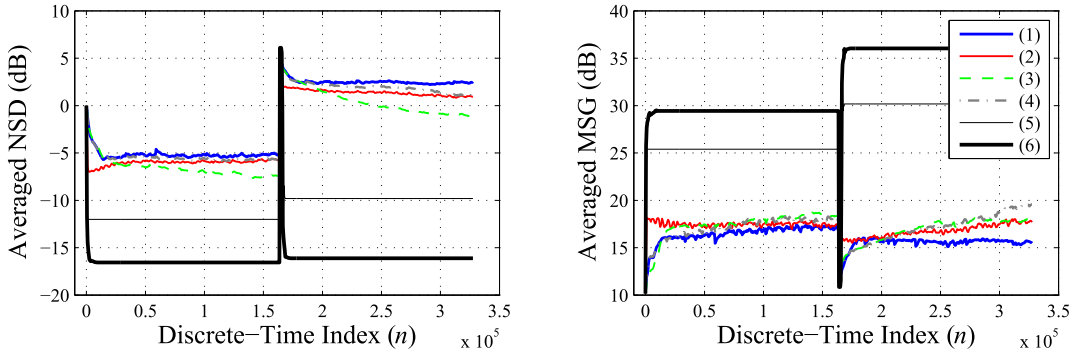

FIGURE 28. Averaged NSD and MSG curves for DHAid with gain $K = 10$ in Case 3 for a sudden change in the acoustic path. [(1) Conventional NLMS AFC, (2) Probe-shaping AFC, (3) PEM-AFC, (4) Basic method, (5) Proposed-a method, and (6) Proposed-b method.]

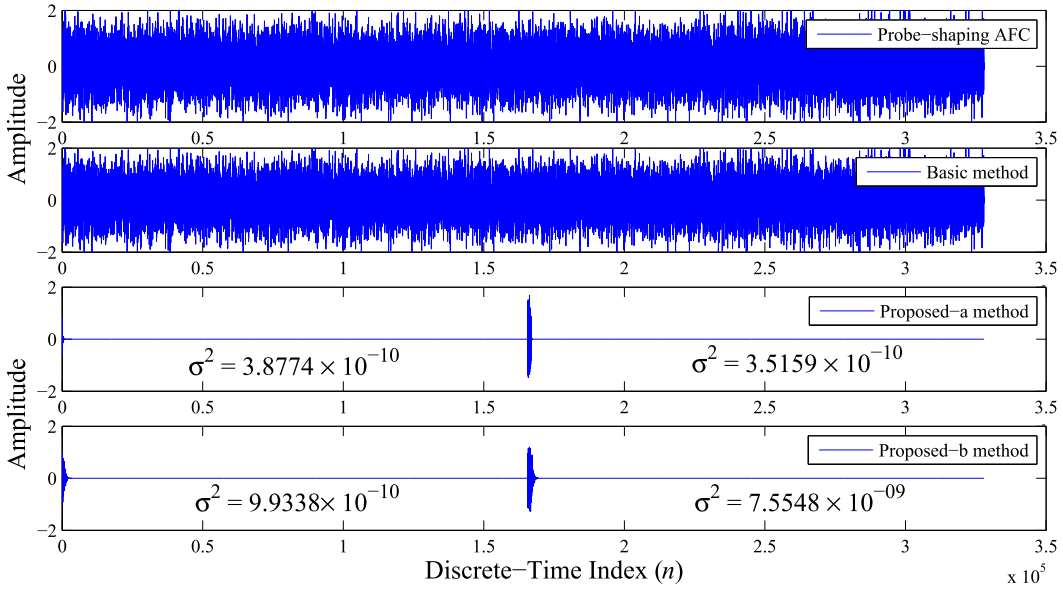

FIGURE 29. Variation of probe signal $p(n)$ in probe signal-based methods for signal S5 in Case 3 for a sudden change in the acoustic path with gain $K = 10$.

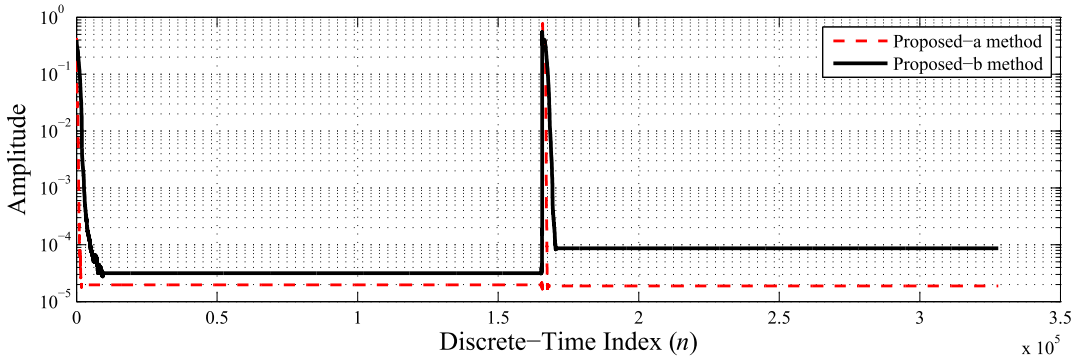

FIGURE 30. Variation of the gain control parameter $\beta(n)$ in proposed method averaged over all signals in Case 3 for a sudden change in the acoustic path with gain $K = 10$.

on the ear. In the simulation results presented in this case study, the experiments for signals in Case 2 for DHAid gain $K = 10$ have been repeated for a situation that $F_1(z)$ is used at the startup at $n = 0$. Later, at the middle of simulation, the acoustic path suddenly changes to $F_2(z)$.

Fig. 26 shows AD (34) curves for the input signal S5. It is observed that the proposed method keeps the good performance before as well as after the sudden change in the acoustic feedback path. The corresponding curves (of impulse response and magnitude response) for estimated acoustic

feedback path $\hat{F}_2(z)$ in comparison with the true one $F_2(z)$, obtained at the end of simulation for various AFC methods are shown in Fig. 27. The existing methods exhibit suboptimal performance especially after the sudden change in acoustic path. On the other hand, the proposed method keeps good performance with proposed-b method showing somewhat better identification of acoustic feedback path in comparison with that of the proposed-a one. The NSD and MSG curves averaged over all signals S1-S7 are presented in Fig. 28, which shows the proposed method outperforms the rest of methods discussed in this paper. A key advantage of the proposed method is automatic tuning of the probe signal to improve upon the steady-state SNR_out. This is demonstrated in Figs. 29 and 30 which show variation of probe signal in all probe signal-based methods (for signal S5) and variation of probe signal gain control parameter $\beta(n)$ (averaged over all signals S1-S7) in the proposed method(s), respectively. It is indeed observed that in contrast to the existing methods using a constant level probe signal, the probe signal level in the proposed method(s) is set to a large value during the transient state and reduces to a very low level (see variances shown in the Fig. 29 before and after sudden change in the acoustic path). This is thanks to the gain control strategy incorporated in the proposed method(s). As shown in Fig. 30, the gain control parameter is tuned to a large value at the start-up and when a sudden change in the acoustic path is detected, and it converges to a very small value as the AFC system converges.

V. CONCLUSION

This paper has investigated a time-domain fully adaptive method for AFC in DHAid devices. In contrast to classical PEM-AFC, which is based on performing AR modeling at regular intervals, the proposed method employs lattice adaptive filtering on the basis of sample-by-sample processing. It is demonstrated by extensive simulations that the proposed method gives very effective performance both for speech as well as audio signal having musical and/or tonal characteristics. Furthermore, the proposed method exhibits robust performance for changes in the acoustic environment. The next important direction of work is to exploit the feature LMS adaptation [57] in the framework of proposed method and target when the acoustic feedback path exhibits sparse characteristics which is typically the case in many practical scenarios.

REFERENCES

[1] World Health Organization. (2020). *Deafness and Hearing Loss*. [Online]. Available: https://www.who.int/news-room/fact-sheets/detail/deafness-and-hearing-loss
[2] H. Amieva, C. Ouvrard, C. Meillon, L. Rullier, and J.-F. Dartigues, "Death, depression, disability, and dementia associated with self-reported hearing problems: A 25-year study," *J. Gerontol., A*, vol. 73, no. 10, pp. 1383–1389, Sep. 2018.
[3] H. Amieva, C. Ouvrard, C. Giulioli, C. Meillon, L. Rullier, and J.-F. Dartigues, "Self-reported hearing loss, hearing aids, and cognitive decline in elderly adults: A 25-year study," *J. Amer. Geriatrics Soc.*, vol. 63, no. 10, pp. 2099–2104, Oct. 2015, doi: 10.1111/JGS.13649.
[4] Y.-C. Lin, Y.-H. Lai, H.-W. Chang, Y. Tsao, Y.-P. Chang, and R. Y. Chang, "SmartHear: A smartphone-based remote microphone hearing assistive system using wireless technologies," *IEEE Syst. J.*, vol. 12, no. 1, pp. 20–29, Mar. 2018.
[5] J. García-Gómez, R. Gil-Pita, M. Aguilar-Ortega, M. Utrilla-Manso, M. Rosa-Zurera, and I. Mohino-Herranz, "Linear detector and neural networks in cascade for voice activity detection in hearing aids," *Appl. Acoust.*, vol. 175, Apr. 2021, Art. no. 107832.
[6] S. Kochkin, "Marketrak VII: Customer satisfaction with hearing instruments in the digital age," *Hear. J.*, vol. 58, no. 9, pp. 30–43, 2005.
[7] H. Dillon, *Hearing Aids*, 2nd ed. New York, NY, USA: Thieme, 2012.
[8] M. C. Killion, "The hollow voice occlusion effect," in *Proc. 13th Danavox Symp.*, 1988, pp. 231–241.
[9] D. K. Bustamante, T. L. Worrall, and M. J. Williamson, "Measurement and adaptive suppression of acoustic feedback in hearing aids," in *Proc. Int. Conf. Acoust., Speech, Signal Process.*, 1989, pp. 2017–2020.
[10] J. M. Kates, *Digital Hearing Aids*, San Diego, CA, USA: Plural Publishing, 2008.
[11] J. Hellgren, "Analysis of feedback cancellation in hearing aids with filtered-X LMS and the direct method of closed loop identification," *IEEE Trans. Speech Audio Process.*, vol. 10, no. 2, pp. 119–131, Feb. 2002.
[12] M. T. Akhtar and D. Banjerdpongchai, "Howling and entrainment in hearing aids: A review," *Eng. J.*, vol. 20, no. 5, pp. 5–13, Nov. 2016, doi: 10.4186/EJ.2016.20.5.5.
[13] A. Schasse, T. Gerkmann, R. Martin, W. Sörgel, T. Pilgrim, and H. Puder, "Two-stage filter-bank system for improved single-channel noise reduction in hearing aids," *IEEE/ACM Trans. Audio, Speech, Language Process.*, vol. 23, no. 2, pp. 383–393, Feb. 2015.
[14] S. C. Douglas, "A family of normalized LMS algorithms," *IEEE Signal Process. Lett.*, vol. 1, no. 3, pp. 49–51, Mar. 1994.
[15] P. Estermann and A. Kaelin, "Feedback cancellation in hearing aids: Results from using frequency-domain adaptive filters," in *Proc. IEEE Int. Symp. Circuits Syst.*, May 1994, pp. 257–260.
[16] A. Spriet, I. Proudler, M. Moonen, and J. Wouters, "Adaptive feedback cancellation in hearing aids with linear prediction of the desired signal," *IEEE Trans. Signal Process.*, vol. 53, no. 10, pp. 3749–3763, Oct. 2005.
[17] G. Rombouts, T. Van Waterschoot, and M. Moonen, "Robust and efficient implementation of the PEM-AFROW algorithm for acoustic feedback cancellation," *J. Audio Eng. Soc.*, vol. 55, no. 11, pp. 955–966, 2007.
[18] A. Spriet, S. Doclo, M. Moonen, and J. Wouters, "Feedback control in hearing aids," in *Springer Handbook of Speech Processing*, J. Benesty, M. Sondhi, and Y. Huang, Eds. Berlin, Germany: Springer, 2008, pp. 979–1000.
[19] J. E. Greenberg, P. M. Zurek, and M. Brantley, "Evaluation of feedback-reduction algorithms for hearing aids," *J. Acoust. Soc. Amer.*, vol. 108, no. 5, pp. 2366–2376, Nov. 2000.
[20] M. Guo, S. H. Jensen, and J. Jensen, "Novel acoustic feedback cancellation approaches in hearing aid applications using probe noise and probe noise enhancement," *IEEE Trans. Audio, Speech, Language Process.*, vol. 20, no. 9, pp. 2549–2563, Nov. 2012.
[21] C. R. C. Nakagawa, S. Nordholm, and W.-Y. Yan, "Feedback cancellation with probe shaping compensation," *IEEE Signal Process. Lett.*, vol. 21, no. 3, pp. 365–369, Mar. 2014.
[22] R. Vicen-Bueno, A. Martinez-Leira, R. Gil-Pita, and M. Rosa-Zurera, "Modified LMS-based feedback-reduction subsystems in digital hearing aids based on WOLA filter bank," *IEEE Trans. Instrum. Meas.*, vol. 58, no. 9, pp. 3177–3190, Sep. 2009.
[23] C. R. C. Nakagawa, S. Nordholm, and W.-Y. Yan, "Dual microphone solution for acoustic feedback cancellation for assistive listening," in *Proc. IEEE Int. Conf. Acoust., Speech Signal Process. (ICASSP)*, Mar. 2012, pp. 149–152.
[24] C. R. C. Nakagawa, S. Nordholm, and W.-Y. Yan, "Analysis of two microphone method for feedback cancellation," *IEEE Signal Process. Lett.*, vol. 22, no. 1, pp. 35–39, Jan. 2015.
[25] S. A. Khoubrouy and I. Panahi, "A method of howling detection in presence of speech signal," *Signal Process.*, vol. 119, pp. 153–161, Feb. 2016.
[26] M. T. Akhtar and A. Nishihara, "Automatic tuning of probe noise for continuous acoustic feedback cancelation in hearing aids," in *Proc. 24th Eur. Signal Process. Conf. (EUSIPCO)*, Budapest, Hungary, Aug. 2016, pp. 888–892.
[27] M. T. Akhtar, F. Albu, and A. Nishihara, "Acoustic feedback cancellation in hearing aids using dual adaptive filtering and gain-controlled probe signal," *Biomed. Signal Process. Control*, vol. 52, pp. 1–13, Jul. 2019.

[28] M. T. Akhtar, F. Albu, and A. Nishihara, "Maximum Versoria-criterion (MVC)-based adaptive filtering method for mitigating acoustic feedback in hearing-aid devices," *Appl. Acoust.*, vol. 181, Oct. 2021, Art. no. 108156, doi: 10.1016/J.APACOUST.2021.108156.

[29] G. Rombouts, T. V. Waterschoot, K. Struyve, and M. Moonen, "Acoustic feedback cancellation for long acoustic paths using a nonstationary source model," *IEEE Trans. Signal Process.*, vol. 54, no. 9, pp. 3426–3434, Sep. 2006.

[30] A. Spriet, G. Rombouts, M. Moonen, and J. Wouters, "Adaptive feedback cancellation in hearing aids," *J. Franklin Inst.*, vol. 343, no. 6, pp. 545–573, Aug. 2006.

[31] J. M. Gil-Cacho, T. van Waterschoot, M. Moonen, and S. H. Jensen, "Wiener variable step size and gradient spectral variance smoothing for double-talk-robust acoustic echo cancellation and acoustic feedback cancellation," *Signal Process.*, vol. 104, pp. 1–14, Nov. 2014.

[32] G. Bernardi, T. van Waterschoot, J. Wouters, and M. Moonen, "Adaptive feedback cancellation using a partitioned-block frequency-domain Kalman filter approach with PEM-based signal prewhitening," *IEEE/ACM Trans. Audio, Speech, Language Process.*, vol. 25, no. 9, pp. 1480–1494, Sep. 2017.

[33] S. Nordholm, H. Schepker, L. T. T. Tran, and S. Doclo, "Stability-controlled hybrid adaptive feedback cancellation scheme for hearing aids," *J. Acoust. Soc. Amer.*, vol. 143, no. 1, pp. 150–166, Jan. 2018.

[34] F. Albu, L. T. T. Tran, and S. Nordholm, "The hybrid simplified Kalman filter for adaptive feedback cancellation," in *Proc. Int. Conf. Commun. (COMM)*, Bucharest, Romania, Jun. 2018, pp. 45–50.

[35] B. Farhang-Boroujeny, *Adaptive Filters: Theory and Applications*, 2nd ed. Hoboken, NJ, USA: Wiley, 2013.

[36] M. T. Akhtar and A. Nishihara, "Lattice adaptive filtering-based method for acoustic feedback cancellation in hearing aids with robustness against sudden changes in the feedback path," in *Proc. 8th Int. Workshop Signal Design Appl. Commun. (IWSDA)*, Sapporo, Japan, Sep. 2017, pp. 59–63.

[37] A. Mader, H. Puder, and G. U. Schmidt, "Step-size control for acoustic echo cancellation filters—An overview," *Signal Process.*, vol. 80, no. 9, pp. 1697–1719, Sep. 2000.

[38] F. Huang, J. Zhang, and S. Zhang, "Maximum Versoria criterion-based robust adaptive filtering algorithm," *IEEE Trans. Circuits Syst. II, Exp. Briefs*, vol. 64, no. 10, pp. 1252–1256, Oct. 2017.

[39] M. T. Akhtar, "On reducing effect of acoustic feedback in hearing aids by employing lattice prediction and hybrid adaptive filtering," in *Proc. IEEE 10th Annu. Inf. Technol., Electron. Mobile Commun. Conf. (IEMCON)*, Vancouver, BC, Canada, Oct. 2019, pp. 878–884.

[40] M. G. Siqueira and A. Alwan, "Steady-state analysis of continuous adaptation in acoustic feedback reduction systems for hearing-aids," *IEEE Trans. Speech Audio Process.*, vol. 8, no. 4, pp. 443–453, Jul. 2000.

[41] L. T. T. Tran, S. E. Nordholm, H. Schepker, H. H. Dam, and S. Doclo, "Two-microphone hearing aids using prediction error method for adaptive feedback control," *IEEE/ACM Trans. Audio, Speech, Language Process.*, vol. 26, no. 5, pp. 909–923, May 2018.

[42] B. Bispo, C. Yamamura, W. Nogueira, E. Theodoro, and P. Rodrigues, "Analysis of acoustic feedback cancellation systems based on direct closed-loop identification," *J. Commun. Inf. Syst.*, vol. 35, no. 1, pp. 217–229, 2020.

[43] M. Hayes, *Statistical Digital Signal Processing and Modeling*. Hoboken, NJ, USA: Wiley, 1996.

[44] M. T. Akhtar and A. Nishihara, "Acoustic feedback neutralization in digital hearing aids—A two adaptive filters-based solution," in *Proc. IEEE Int. Symp. Circuits Syst. (ISCAS)*, Beijing, China, May 2013, pp. 529–532.

[45] H. Garudadri, A. Boothroyd, C.-H. Lee, S. Gadiyaram, J. Bell, D. Sengupta, S. Hamilton, K. C. Vastare, R. Gupta, and B. D. Rao, "A realtime, open-source speech-processing platform for research in hearing loss compensation," in *Proc. 51st Asilomar Conf. Signals, Syst., Comput.*, Oct. 2017, pp. 1900–1904.

[46] J. Alexander, "Hearing aid delay and current drain in modern digital devices," *Can. Audiologist*, vol. 3, no. 4, pp. 1–15, 2016. [Online]. Available: https://canadianaudiologist.ca/hearing-aid-delay-feature/

[47] P. C. Loizou, *Speech Enhancement Theory and Practice*. Boca Raton, FL, USA: CRC Press, 2007.

[48] A. J. Manders, D. M. Simpson, and S. L. Bell, "Objective prediction of the sound quality of music processed by an adaptive feedback canceller," *IEEE Trans. Audio, Speech, Language Process.*, vol. 20, no. 6, pp. 1734–1745, Aug. 2012.

[49] Å. Olofsson and M. Hansen, "Objectively measured and subjectively perceived distortion in nonlinear systems," *J. Acoust. Soc. Amer.*, vol. 120, no. 6, pp. 3759–3769, Dec. 2006.

[50] E. Vincent, R. Gribonval, and C. Fevotte, "Performance measurement in blind audio source separation," *IEEE Trans. Audio, Speech, Language Process.*, vol. 14, no. 4, pp. 1462–1469, Jul. 2006.

[51] A. Hyvärinen and E. Oja, "Independent component analysis: Algorithms and applications," *Neural Netw.*, vol. 13, nos. 4–5, pp. 411–430, Jun. 2000.

[52] J. M. Kates and K. H. Arehart, "The hearing-aid speech quality index (HASQI)," *J. Audio Eng. Soc.*, vol. 58, no. 5, pp. 363–381, 2010.

[53] J. Kates and K. Arehart, "The hearing-aid speech quality index (HASQI) version 2," *J. Audio Eng. Soc.*, vol. 62, no. 3, pp. 99–117, Mar. 2014.

[54] J. M. Kates and K. H. Arehart, "The hearing-aid audio quality index (HAAQI)," *IEEE/ACM Trans. Audio, Speech, Language Process.*, vol. 24, no. 2, pp. 354–365, Feb. 2016.

[55] Y. Hu and P. C. Loizou, "Subjective comparison and evaluation of speech enhancement algorithms," *Speech Commun.*, vol. 49, nos. 7–8, pp. 588–601, Jul. 2007.

[56] H. P. Natarajan and J. S. Kindred, "Method and apparatus to reduce entrainment-related artifacts for hearing assistance systems," U.S. Patent 2011/0 116 667 A1, May 19, 2011.

[57] H. Yazdanpanah, P. S. R. Diniz, and M. V. S. Lima, "Feature adaptive filtering: Exploiting hidden sparsity," *IEEE Trans. Circuits Syst. I, Reg. Papers*, vol. 67, no. 7, pp. 2358–2371, Jul. 2020.

MUHAMMAD TAHIR AKHTAR (Senior Member, IEEE) received the B.Sc. degree in electrical electronics and communication engineering from the University of Engineering and Technology, Taxila, Pakistan, in 1997, the M.Sc. degree in systems engineering from Quaid-i-Azam University, Islamabad, Pakistan, in 1999, and the Ph.D. degree in electronic engineering from Tohoku University, Sendai, Japan, in 2004.

From 2004 to 2005, he was a COE Postdoctoral Fellow at Tohoku University, Sendai. From 2006 to 2008, he worked as an Assistant Professor at United Arab Emirates University. From December 2008 to February 2009, he was a Visiting Researcher at the Institute of Sound and Vibration Research (ISVR), University of Southampton, U.K. From 2008 to 2014, he was an Assistant Professor at The University of Electro-Communications, Tokyo, Japan, and a Special Visiting Researcher at the Tokyo Institute of Technology, Tokyo. From November 2010 to March 2011, he was with the Institute for Neural Computations (INC), University of California at San Diego. From 2014 to 2017, he was an Associate Professor at COMSATS University Islamabad, Pakistan. He is currently working as an Associate Professor with the Department of Electrical and Computer Engineering, School of Engineering and Digital Sciences, Nazarbayev University, Astana, Kazakhstan. He has published about 110 papers in the peer-reviewed international journals and conference proceedings. His research interests include adaptive signal processing, active noise control, blind source separation, and biomedical signal processing.

Dr. Akhtar is a member of the IEEE Signal Processing Society and the IEEE Industrial Electronic Society. He won the Best Student Paper at the IEEE 2004 Midwest Symposium on Circuits and Systems, Hiroshima, Japan, and Student Paper Award (with Marko Kanadi) at 2010 RISP International Workshop on Nonlinear Circuits, Communications and Signal Processing. He was on the Editorial Board of *Advances in Mechanical Engineering*, and served (2011–2013) as a Co-Editor for the newsletter of Asia-Pacific Signal and Information Processing Association (APSIPA).

FELIX ALBU (Senior Member, IEEE) received the M.S. degree in applied electronics and the Ph.D. degree in telecommunications from the University Politehnica of Bucharest, Romania, in 1993and May 1999, respectively. He worked as a Teaching Assistant at the University Politehnica of Bucharest, from 1993 to 1999. During his Ph.D. study, he has been a Visiting Researcher for about two years at the National Institute of Telecommunications, Evry, France, and LAAS-CNRS, Toulouse, France. He has obtained extensive research experience as a Postdoctoral Researcher at University College Dublin, Ireland (1999–2002), and the Aristotle University of Thessaloniki, Greece (2004–2005). Also, he has got industrial research experience at Lake Communications, Dublin, from 2002 to 2003 and at Fotonation Romania, from 2006 to 2011. He is currently a Full Professor with the Valahia University of Târgovişte, Romania. His research interests include various signal processing and machine learning areas. Since 2013, he has been a Senior Member of the IEEE SPS. He received the Dr.Habil. certificate in electronics and telecommunications, in 2014.

AKINORI NISHIHARA (Life Fellow, IEEE) received the B.E., M.E., and Dr.Eng. degrees in electronics from the Tokyo Institute of Technology, in 1973, 1975, and 1978, respectively.

Since 1978, he has been with the Department of Physical Electronics, International Cooperation Center for Science and Technology, Center for Research and Development of Educational Technology (CRADLE), and Department of Human System Science, Tokyo Institute of Technology. He retired, in 2016, but was rehired by the Human Assets Promotion Program for Innovative Education and Research (HAPPIER), Tokyo Institute of Technology. Since 2019, he has been serving as a COO of Tokyo Tech Academy for Super Smart Society. He has published more than 300 technical papers in refereed international journals and conferences. His research interests include signal processing and educational technology.

Dr. Nishihara received the Best Paper Awards from the IEEE Asia-Pacific Conference on Circuits and Systems, in 1994 and 2000, the Best Paper Award of the IEICE in 1999, and the IEEE Third Millennium Medal in 2000. He also received a 4th LSI IP Design Award, in 2002, the Distinguished Service Award for IEEE Student Activities, in 2006, the Best Teacher Award from Tokyo Institute of Technology, in 2009, the Best Engineering Teacher Award, Tokyo Institute of Technology, in 2014, the IEEE Region ten Outstanding Volunteer Award, in 2015, the Commendation for Science and Technology by the Minister of Education, Culture, Sports, Science and Technology, in 2016, the IEICE Excellent Educational Practices Award, in 2017, and was selected as an Extraordinary Man, in 2022, in the IEEE WIE's 25th Anniversary Celebration. He was the Chair of the IEICE Technical Group on Circuits and Systems, from 1997 to 1998. He served as the IEICE Director of Conferences, Student Activities and Education, during 2007–2009, the Director of General Affairs, during 2011–2013, and an Auditor 2020–2022. He has been serving on IEEE Region 10 Executive Committee, as the Student Activities Committee Chair (1996–1996), a Treasurer (1999–2000), a Educational Activities Committee Chair (2001–2004), a Strategic Planning Coordinator (2007–2010), a History Coordinator (2016), a Director-Elect (2017–2018), and a member of IEEE Board of the Directors as Region 10 Director (2019–2020). He served as an Associate Editor for the *IEICE Transactions on Fundamentals of Electronics, Communications and Computer Sciences*, from 1990 to 1994, and then an Associate Editor for the *Transactions of IEICE Part A* (in Japanese), from 1994 to 1998. He was an Associate Editor of the IEEE TRANSACTIONS ON CIRCUITS AND SYSTEMS—II: EXPRESS BRIEFS, from 1996 to 1997, and the Editor-in-Chief of *Transactions of IEICE Part A* (in Japanese), from 1998 to 2000.